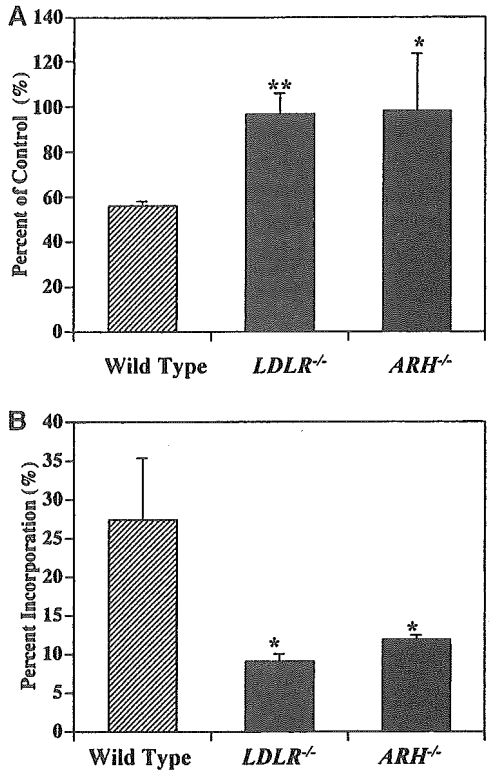

Figure 4. Hepatic uptake of intravenously injected ^{3}H-CE-LDL. ^{3}H-CE-LDL was injected into a mouse of each genotype. The blood was collected at 2 minutes and 4 hours after the injection. Immediately after the blood collection at 4 hours, 2 mg of LDL was injected and equilibrated for 10 minutes. The blood was washed from the body as described in the Methods section, and the liver was isolated. Lipid was extracted from the liver and the blood, and radioactivity was counted. Values are mean±SEM. A, Percentage of remaining tritium radioactivity in the mouse blood after 4 hours compared to that after 2 minutes. B, Hepatic uptake of tritium in the liver, 4 hours after injection, expressed as percentage of the total radioactivity injected calculated from the count in the blood at 2 minutes after the injection. *P<0.05, **P<0.01.

DiI-LDL was monitored. The fluorescence was recovered in the cytosols of both hepatocytes and Kupffer cells of wild-type mice (Figure 3A), and the fluorescence in the hepatocytes was suppressed by pretreatment with excess amounts of LDL (Figure 3C), suggesting that DiI-LDL was incorporated into the hepatocytes via the LDLR. Lower levels of DiI-LDL were found in hepatocytes of *LDLR*$^{-/-}$ and *ARH*$^{-/-}$ mice (Figure 3E, I). Because LDL cholesterol levels were higher in *ARH*$^{-/-}$ mice (1.01±0.21 mmol/L in male, 1.46±0.44 mmol/L in female) than that in wild-type mice (0.17±0.05 mmol/L in male, 0.30±0.04 mmol/L in female), injected DiI-LDL may become more diluted in *ARH*$^{-/-}$ by their own LDL. However, hepatic DiI-LDL uptake in *ARH*$^{-/-}$ mice was much lower than the observed uptake in wild-type mice when the excess LDL was given to raise LDL cholesterol (11.42±1.09 mmol/L). This indicates that the lower uptake of DiI-LDL in *ARH*$^{-/-}$ was not attributable to a dilution effect caused by their high LDL levels (Figure 3C, I).

Small numbers of cells appeared highly fluorescence-positive in the liver of mice of all the genotypes including *LDLR*$^{-/-}$ (Figure 3A, E, I). Their fluorescent activity was not

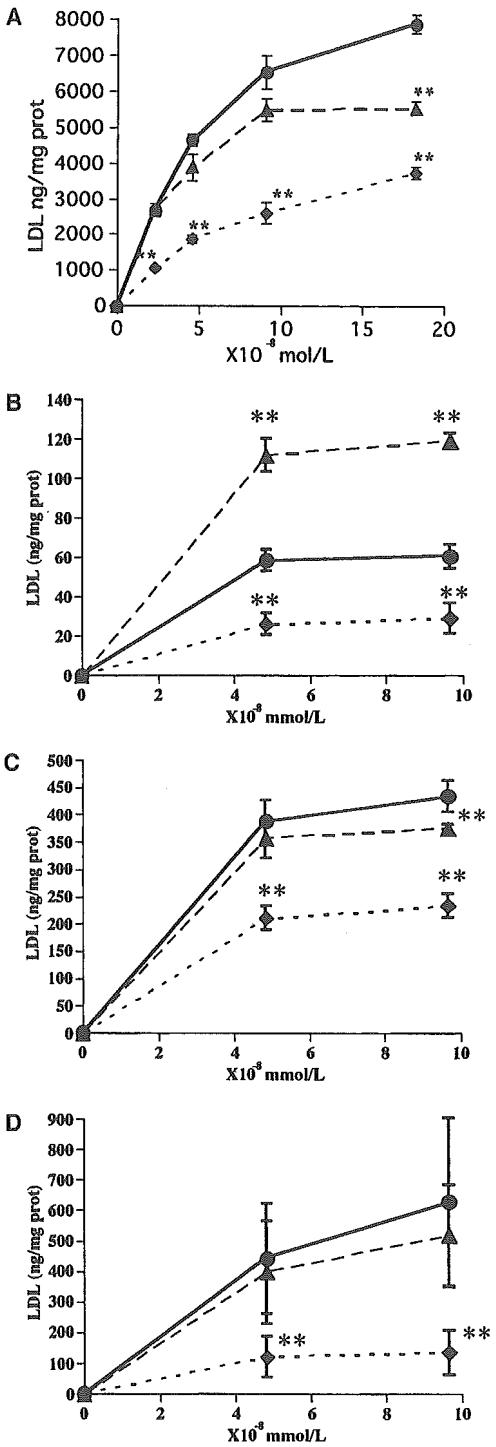

Figure 5. LDL receptor assay in primary cultured hepatocytes. Hepatocytes were obtained from the wild-type, *ARH*$^{-/-}$, and *LDLR*$^{-/-}$ mice, and cultured in Waymouth medium containing 10% fetal calf serum (day 0). On day 2, the medium was removed and the cells were washed twice. Then, the cells were cultured in Waymouth medium containing 10% LPDS. On day 3, the cells were subjected to LDL receptor assay. The data are shown as the mean±SEM of quadruplicate assays. The experiments were performed in the presence of 20-fold excess of LDL for nonspecific binding. A, ^{3}H-CE-LDL incorporation of primary cultured hepatocytes from wild-type (●), *LDLR*$^{-/-}$ (♦), and *ARH*$^{-/-}$ (▲) mice. *P<0.05, **P<0.01 vs wild-type. B, ^{125}I-LDL binding of primary cultured hepatocytes. C, ^{125}I-LDL incorporation of primary cultured hepatocytes. D, ^{125}I-LDL degradation of primary cultured hepatocytes.

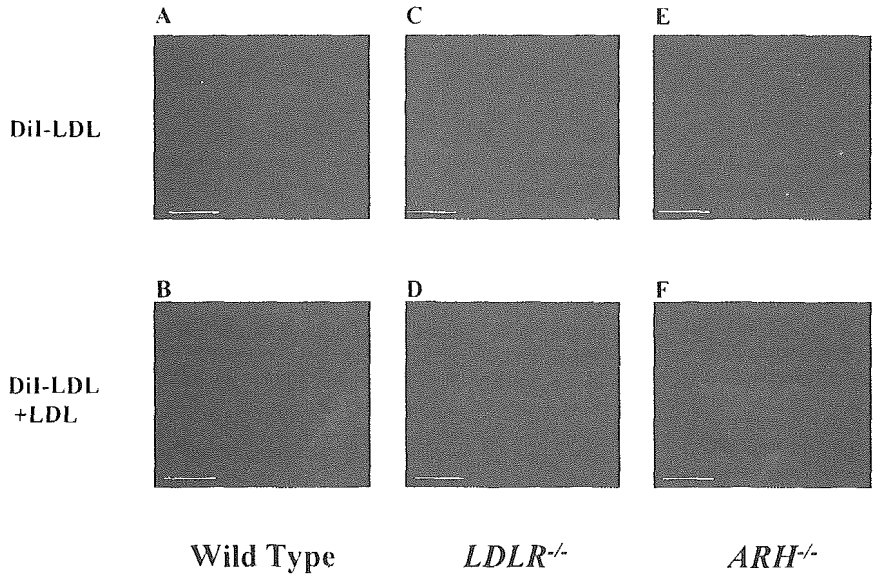

Figure 6. DiI-LDL incorporation in primary cultured hepatocytes of wild-type, $LDLR^{-/-}$, and $ARH^{-/-}$ mice. On day 0, hepatocytes were obtained from wild-type, $ARH^{-/-}$, and $LDLR^{-/-}$ mice, and cultured in Waymouth medium containing 10% fetal calf serum. After 4 hours, the cells were washed with PBS and cultured in Waymouth medium containing 10% LPDS. On day 2, the cells were incubated with DiI-LDL with or without 20 times excess of LDL for 3 hours. Then the cells were washed with PBS and mounted. A, C, and E, Hepatocytes from each genotype of mouse incubated with DiI-LDL. B, D, and F, Hepatocytes from each genotype of mouse incubated with DiI-LDL and excess of LDL. The scale bar indicates 10 μm.

decreased by the presence of excess amounts of LDL (Figure 3C, G, K) and these cells were positively identified as Kupffer cells by immunostaining with the antibody against mouse macrophages (Figure 3B, D, F, H, J, L). Thus, DiI-LDL was incorporated into Kupffer cells via an LDLR-independent pathway.

Hepatic uptake of LDL in $ARH^{-/-}$ was also examined by measuring the uptake of ^{3}H-CE-LDL by the liver. The tritium count in the blood decreased significantly in the wild-type mice, whereas it did not change in $LDLR^{-/-}$ and $ARH^{-/-}$ mice (Figure 4A). This is in agreement with the ^{125}I-LDL turnover study (Figure 2). The incorporation of ^{3}H-CE-LDL into the liver of $LDLR^{-/-}$ and $ARH^{-/-}$ mice was significantly lower than that of the wild-type mice (Figure 4B), suggesting again that the delayed turnover of LDL in $ARH^{-/-}$ mice is attributable to low LDL uptake by the liver. Interestingly, incorporation of ^{3}H-CE-LDL into the liver of $ARH^{-/-}$ is significantly higher than that of $LDLR^{-/-}$ ($P<0.05$). This result implies that the LDLR may function to incorporate LDL in the liver to some extent in vivo even without ARH.

To examine in vitro LDLR activity in the cells of $ARH^{-/-}$ mice, the incorporation of ^{3}H-CE-LDL was measured in primary cultured hepatocytes of $ARH^{-/-}$, $LDLR^{-/-}$, and wild-type mice (Figure 5A). The cultured hepatocytes of $ARH^{-/-}$ incorporated a slightly smaller amount of ^{3}H-CE-LDL than that of the wild-type, but much larger than that of $LDLR^{-/-}$. These findings were confirmed by ^{125}I-LDL incorporation and degradation experiments (Figure 5C, D). The binding of ^{125}I-LDL to the hepatocytes of $ARH^{-/-}$ was larger than that of wild-type (Figure 5B). Recently, Michaely et al[26] reported that the number of LDLRs on the cell surface of the lymphocytes in ARH subject was increased 20-fold, and that LDL binding activity was increased two-fold. The hepatocytes of $ARH^{-/-}$ seemed to remain the characteristics of in vivo status to some extent. To see whether LDL is incorporated into the cell or whether it remains on the cell surface, the cells were incubated with DiI-LDL and observed by using a laser confocal microscopy. The cytosol of the hepatocytes of $ARH^{-/-}$ mice was fluorescently stained, suggesting that DiI-LDL was internalized, like that of wild-type mice (Figure 6A, E). The results were highly consistent with the findings that the LDLR in the cultured fibroblasts from the homozygous ARH patients normally functioned, despite the fact that LDL clearance in their blood was severely impaired.[5] This suggests that the LDLR functions normally in vitro without ARH protein.

The PTB domain of ARH protein has been shown, by pull-down technique, to bind to the FDNPVY sequence of the LDLR protein.[8] ARH protein was also reported to interact with clathrin and AP-2, and it is suggested to function as an adaptor protein that couples LDLR to the endocytic machinery. ARH patients have severe hypercholesterolemia caused by delayed LDL clearance in vivo, although they have normal or subnormal levels of LDLR activity in their fibroblasts when measured in vitro.[5] However, transformed lymphocytes and monocyte-derived macrophages were unable to internalize LDL in ARH patients.[12] Thus, the dependency of LDLR function on ARH protein can be cell-specific. However, we have demonstrated here that hepatocytes do not take-up LDL in vivo without ARH protein, but they normally catabolize LDL in vitro. Thus, the requirement of ARH protein for proper functioning of the LDLR is not cell-specific, but rather may depend on the cellular environment.

Hepatic uptake of ^{3}H-CE from LDL was shown to be significantly higher in $ARH^{-/-}$ mice than $LDLR^{-/-}$ mice. This may indicate that LDLR functions to some extent without ARH, even in vivo. Some other adaptor proteins may compensate for ARH by forming an LDLR–clathrin complex, or the condition can be induced so LDLRs can be internalized without forming a clathrin complex. Our in vitro results strongly indicate that these possibilities may be enabled in a certain cellular environments.

Acknowledgments

This work was supported in part by the Promotion of Fundamental Studies in Health Science of the Organization for Pharmaceutical Safety and Research (OPSR); Research on Advanced Medical Technology from the Ministry of Health, Labour, and Welfare; Ono Medical Research Foundation; Takeda Medical Research Founda-

tion; and grant-in-aid for Scientific Research (C) (No. 15590964) from the Ministry of Education, Science, Sports, and Culture, Japan. We thank Drs Kenji Kangawa, Hisayuki Matsuo, and Hitonobu Tomoike for their helpful discussion and advice, Dr Michitaka Masuda for taking the photograph, and Dr Patrick Leahy for proofreading this manuscript. We also thank Moto Ohira, Eri Abe, Ritsuko Maeda, and Keiko Jinno for their excellent technical assistance.

References

1. Khachadurian AK, Uthman SM. Experiences with the homozygous cases of familial hypercholesterolemia. A report of 52 patients. *Nutr Metab.* 1973;15:132–140.
2. Brown MS, Anderson RG, Basu SK, Goldstein JL. Recycling of cell-surface receptors: observations from the LDL receptor system. *Cold Spring Harb Symp Quant Biol.* 1982;46(Pt 2):713–721.
3. Goldstein JL, Hobbs HH, Brown MS. Familial hypercholesterolemia. In: Scriver CR, Beaudet AL, Sly WS, Valle D, eds. *The Metabolic and Molecular Bases of Inherited Disease.* 8th ed., Vol II. New York: McGraw-Hill; 2001:2863–2913.
4. Harada-Shiba M, Tajima S, Miyake Y, Kojima S, Tsushima M, Yamamoto A. Severe hypercholesterolemia patients with normal LDL receptor. *J Jpn Atheroscler Soc.* 1991;19:227–242.
5. Harada-Shiba M, Tajima S, Yokoyama S, Miyake Y, Kojima S, Tsushima M, Kawakami M, Yamamoto A. Siblings with normal LDL receptor activity and severe hypercholesterolemia. *Arterioscler Thromb.* 1992;12:1071–1078.
6. Garcia CK, Wilund K, Arca M, Zuliani G, Fellin R, Maioli M, Calandra S, Bertolini S, Cossu F, Grishin N, Barnes R, Cohen JC, Hobbs HH. Autosomal recessive hypercholesterolemia caused by mutations in a putative LDLR adaptor protein. *Science.* 2001;292:1394–1398.
7. Harada-Shiba M, Takagi A, Miyamoto Y, Tsushima M, Ikeda Y, Yokoyama S, Yamamoto A. Clinical features and genetic analysis of autosomal recessive hypercholesterolemia. *J Clin Endocrinol Metab.* 2003;88:2541–2547.
8. He G, Gupta S, Yi M, Michaely P, Hobbs HH, Cohen JC. ARH is a modular adaptor protein that interacts with the LDL receptor, clathrin, and AP-2. *J Biol Chem.* 2002;277:44044–44049.
9. Schmidt HH, Stuhrmann M, Shamburek R, Schewe CK, Ebhardt M, Zech LA, Buttner C, Wendt M, Beisiegel U, Brewer HB, Jr, Manns MP. Delayed low density lipoprotein (LDL) catabolism despite a functional intact LDL-apolipoprotein B particle and LDL-receptor in a subject with clinical homozygous familial hypercholesterolemia. *J Clin Endocrinol Metab.* 1998;83:2167–2174.
10. Zuliani G, Arca M, Signore A, Bader G, Fazio S, Chianelli M, Bellosta S, Campagna F, Montali A, Maioli M, Pacifico A, Ricci G, Fellin R. Characterization of a new form of inherited hypercholesterolemia: familial recessive hypercholesterolemia. *Arterioscler Thromb Vasc Biol.* 1999;19:802–809.
11. Zuliani G, Vigna GB, Corsini A, Maioli M, Romagnoni F, Fellin R. Severe hypercholesterolaemia: unusual inheritance in an Italian pedigree. *Eur J Clin Invest.* 1995;25:322–331.
12. Norman D, Sun XM, Bourbon M, Knight BL, Naoumova RP, Soutar AK. Characterization of a novel cellular defect in patients with phenotypic homozygous familial hypercholesterolemia. *J Clin Invest.* 1999;104:619–628.
13. Eden ER, Patel DD, Sun XM, Burden JJ, Themis M, Edwards M, Lee P, Neuwirth C, Naoumova RP, Soutar AK. Restoration of LDL receptor function in cells from patients with autosomal recessive hypercholesterolemia by retroviral expression of ARH1. *J Clin Invest.* 2002;110:1695–1702.
14. Jones C, Hammer RE, Li WP, Cohen JC, Hobbs HH, Herz J. Normal sorting but defective endocytosis of the low density lipoprotein receptor in mice with autosomal recessive hypercholesterolemia. *J Biol Chem.* 2003;278:29024–29030.
15. Usui S, Hara Y, Hosaki S, Okazaki M. A new on-line dual enzymatic method for simultaneous quantification of cholesterol and triglycerides in lipoproteins by HPLC. *J Lipid Res.* 2002;43:805–814.
16. Zambrowicz BP, Friedrich GA, Buxton EC, Lilleberg SL, Person C, Sands AT. Disruption and sequence identification of 2,000 genes in mouse embryonic stem cells. *Nature.* 1998;392:608–611.
17. Ishibashi S, Brown MS, Goldstein JL, Gerard RD, Hammer RE, Herz J. Hypercholesterolemia in low density lipoprotein receptor knockout mice and its reversal by adenovirus-mediated gene delivery. *J Clin Invest.* 1993;92:883–893.
18. Sambrook J, Russell DW. *Molecular Cloning: A Laboratory Manual.* Cold Spring Harbor: Cold Spring Harbor Laboratory Press; 2001.
19. Nishimura N, Harada-Shiba M, Tajima S, Sugano R, Yamamura T, Qiang QZ, Yamamoto A. Acquisition of secretion of transforming growth factor-beta 1 leads to autonomous suppression of scavenger receptor activity in a monocyte-macrophage cell line, THP-1. *J Biol Chem.* 1998;273:1562–1567.
20. Bilheimer DW, Eisenberg S, Levy RI. The metabolism of very low density lipoprotein proteins. I. Preliminary in vitro and in vivo observations. *Biochim Biophys Acta.* 1972;260:212–221.
21. Nishikawa O, Yokoyama S, Okabe H, Yamamoto A. Enhancement of non-polar lipid transfer reaction through stabilization of substrate lipid particles with apolipoproteins. *J Biochem (Tokyo).* 1988;103:188–194.
22. Folch J, Lees M, Sloane Stanley GH. A simple method for the isolation and purification of total lipides from animal tissues. *J Biol Chem.* 1957;226:497–509.
23. Seglen PO. Control of glycogen metabolism in isolated rat liver cells by glucose, insulin and glucagon. *Acta Endocrinol Suppl (Copenh).* 1974;191:153–158.
24. Hara H, Yokoyama S. Interaction of free apolipoproteins with macrophages. Formation of high density lipoprotein-like lipoproteins and reduction of cellular cholesterol. *J Biol Chem.* 1991;266:3080–3086.
25. Goldstein JL, Basu SK, Brown MS. Receptor-mediated endocytosis of low-density lipoprotein in cultured cells. *Methods Enzymol.* 1983;98:241–260.
26. Michaely P, Li WP, Anderson RG, Cohen JC, Hobbs HH. The modular adaptor protein ARH is required for low density lipoprotein (LDL) binding and internalization but not for LDL receptor clustering in coated pits. *J Biol Chem.* 2004;279:34023–34031.

High Performance Gene Delivery Polymeric Vector: Nano-Structured Cationic Star Polymers (Star Vectors)

Yasuhide Nakayama[1,*], Takeshi Masuda[1], Makoto Nagaishi[1], Michiko Hayashi[1], Moto Ohira[2] and Mariko Harada-Shiba[2]

[1]*Department of Bioengineering, National Cardiovascular Center Research Institute,* [2]*Department of Bioscience, National Cardiovascular Center Research Institute, 5-7-1 Fujishiro-dai, Suita, Osaka 565-8565, Japan*

Abstract: Nano-structured hyperbranched cationic star polymers, called star vectors, were molecularly designed for a novel gene delivery non-viral vector. The linear and 3, 4 or 6 branched water-soluble cationic polymers, which had same molecular weight of ca. 18,000, were synthesized by iniferter (initiator-transfer agent-terminator)-based photo-living-radical polymerization of 3-(*N,N*-dimethylamino)propyl acrylamide, initiated from respective multi-dithiocarbamate-derivatized benzenes as an iniferter. All polymers produced polyion complexes 'polyplexes' by mixing with pDNA (pGL3-control plasmid), in which the particle size was ca. 250 nm in diameter [the charge ratio < 2/1 (vevtor/pDNA)] and ca. 150 nm (the charge ratio > 2.5/1), and the ζ-potential was ca. +10 mV (the charge ratio > 1/1). When COS-1 cells were incubated with the polyplexes 12h after preparation under the charge ratio of 5/1, higher gene expression was obtained as an increase in branching, with a little cytotoxicity. The relative gene expression to the linear polymer was about 2, 5, and 10 times in 3-, 4-, and 6-branched polymers, respectively. The precise change in branching of polymers enabled the control of the gene transfer activity.

Keywords: Non-viral vector, star polymer, polyplex, branched polymer, gene transfection, molecular design.

INTRODUCTION

The cationic polymers, which can generate nano-particles by formation of polyion complexes 'polyplexes' with DNA irrespective of its size and kind, are highly expected as one of the major materials for non-viral vectors [1-4]. However, the primary obstacle toward implementing an effective gene therapy using the cationic polymers remains their relatively inefficient gene transfection *in vivo* than virus vectors.

To achieve an enhancement of gene transfection using cationic polymers, numerous studies have been performed by various approaches; e.g., the chemical synthetic engineering approach in which the kind and composition of the polymers are modified [5,6], biochemical approach in which targeting ligands such as galactose, mannose, transferring, or antibodies into the polymers [7-11], functional molecular engineering approach in which stimulus-response polymers with light and thermal reactivity are designed as high performance vectors [12-14], and physical engineering approach in which physical stimulation with electroporation, gene gun, ultrasound and hydrodynamic pressure are provided at the transfection [2,15,16]. However, few studies in the molecular structure of cationic polymers, which are usually synthesized by conventional radical polymerization, has been reported, except for the effects of changes in the polymer chain length and composition of polymers [17-20] and complex multi-branching polymers, of which structural analysis is impossible [21-24]. Since precise molecular design, including the molecular weight and three-dimensional structure, by conventional radical polymerization was quite difficult in general, the systematic structure-dependency of cationic polymers in gene transfection has not been established.

In this study, for examination of the effects of the molecular structure on gene expression we designed novel cationic polymers with star-shaped and symmetric structure, which is determined by 2-parameters, the degree of branching and chain length. Molecular design was performed by the iniferter (acts as *ini*tiator-trans*fer* agent-*ter*minator)-based photo-living-radical polymerization method pioneered by Otsu *et al.* [25-30]. An iniferter, benzyl *N,N*-diethyldithiocarbamate (DC) is dissociated into a benzyl radical and a dithiocarbamyl radical by ultraviolet light (UV) irradiation. The reaction involving an *N,N*-diethyldithiocarbamyl radical favors chain termination with a growing polymer chain radical end rather than a reaction with a vinyl monomer, whereas a benzyl radical reacts with a vinyl monomer to produce a polymer. These reactions proceed only during irradiation. Therefore, the chain length of the growing polymer is controlled by irradiation condition such as irradiation time or light intensity and the composition of the solution. We previously used the living radical polymerization for designing of various surface graft architectures [31-34] controlling the chain length, block graft chain, gradient chain length and regionally graft polymerized pattern surface. As the first step of the study, star polymers of the same molecular weight at a precise degree of branching of 0, 3, 4, and 6 were synthesized. The effects of the degree of branching on gene expression by measuring the luciferase activity were examined.

*Address correspondence to this author at the Department of Bioengineering, National Cardiovascular Center Research Institute, 5-7-1 Fujishiro-dai, Suita, Osaka 565-8565, Japan; Tel: +81-6-6833-5012; Fax: +81-6-6872-8090; E-mail: nakayama@ri.ncvc.go.jp

1567-2018/05 $50.00+.00

MATERIALS AND METHODS

Materials

Benzyl chloride, 2,4,6-tris(bromomethyl)mesitylene, 1,2,4,5-tetrakis(bromomethyl)benzene, and hexakis(bromomethyl)benzene were obtained from Sigma-Aldrich (Milwaukee, WI). Sodium *N,N*-diethyldithiocarbamate and *N,N*-dimethyaminopropyl acrylamide were purchased from Wako Pure Chemical Ind. Ltd. (Osaka, Japan). Solvents and other reagents, all of which were of special reagent grade, were obtained from Wako and used after conventional purification. Plasmid DNA (pGL3-control), which contains the firefly luciferase gene, was obtained from Promega Inc., (Tokyo, Japan). ExGen 500 [poly(ethylene imine)] was obtained from Euromedex Inc., (Cedex, France).

Synthesis of Cationic Star Polymers

Cationic polymers including linear and three types of star polymers with 3, 4, or 6 branches per molecule were prepared by iniferter-based photo-living-radical polymerization of 3-(*N,N*-dimethylamino)propyl acrylamide as a monomer from respective inifeters such as benzyl *N,N*-diethyldithiocarbamate, 2,4,6-tris (*N,N*-diethyldithiocarbamylmethyl)mesitylene, 1,2,4,5- tetrakis(*N,N*-diethyldithiocarbamylmethyl)benzene, and hexakis (*N,N*-diethyldithiocarbamylmethyl)benzene, which were obtained by *N,N*-diethyldithiocarbamylation from respective benzyl halogenate derivatives such as benzyl chloride, 2,4,6-tris (bromomethyl)mesitylene, 1,2,4,5-tetrakis(bromomethyl) benzene, and hexakis(bromomethyl)benzene.

The general preparation method of iniferter is followed. An ethanol solution (10 ml) of chloromethyl benzene (4.8 g, 38 mmol) was added to an ethanol solution (50 ml) of sodium *N,N*-diethyldithiocarbamate (10.3 g, 46 mmol) at 0°C. After the mixture was stirred at room temperature for 24 h, the resulting sodium chloride was separated by filtration. The filtrate was concentrated under reduced pressure. The residue was added into 150 ml of water and extracted with ether (200 ml x 2) and washed successively with deionized water (100 ml x 3), followed the separation of the organic layer, drying over $MgSO_4$, condensation to give benzyl *N,N*-diethyldithiocarbamate: yield, 17.6g (93%); ^{1}H NMR (DMSO-d_6 with Me_4Si) δ 7.34 (m, 5H, C_6H_5), 4.54 (s, 2H, CH_2-S), 4.05 (q, 2H, N-CH_2), 3.73 (q, 2H, N-CH_2), 1.28 (m, 6H, CH_2CH_3).

The general procedure of iniferter-induced photo-living-radical polymerization is followed. A methanol solution (20 ml) of benzyl *N,N*-diethyldithiocarbamate (24 mg, 0.1 mmol) and 3-(*N,N*-dimethylamino)propyl acrylamide (3.9 g, 25 mmol) was placed into 50 ml quartz crystal tube. A stream of dry nitrogen was introduced through a gas inlet to sweep the tube for 5 min or more. The solution was then irradiated for 30 min with a 200 W Hg lamp (SPOT CURE, USHIO, Tokyo, Japan) in nitrogen atmosphere at 20~25 °C. Light intensity was set to 1 mW/cm^2 at the wavelength of 250 nm (UVR-1, TOPCON, Tokyo, Japan). The reaction mixture was concentrated under reduced pressure. The residue was dissolved in a small amount of methanol. The precipitate, obtained by the addition of a large amount of ether, was separated by filtration. Reprecipitation was performed in the methanol-ether system. The last precipitate was dried in a vacuum to yield poly[3-(*N, N*-dimethylamino)propyl acrylamide] as a white powder. The molecular weight, determined by GPC analysis, was 18,000 g mol^{-1}. ^{1}H NMR (DMSO-d_6 with Me_4Si) δ 7.60 (br, 1H, N-*H*), 3.22 (br, 2H, NH-CH_2), 2.30 ((br, 2H, $N(CH_3)_2$-CH_2), 2.15 (br, 6H, N-CH_3), 1.65 (br, 2H, CH_2-CH_2).

General Methods

GPC analysis was carried out on a RI-8012 (TSK_{gel} α-3000 and α-5000; Tosoh, Tokyo, Japan) after calibration with standard polyethylene glycol samples. The eluent was *N,N*-dimethylformamide. ^{1}H-NMR spectra were obtained on a Valian Gemini-300 (300 MHz) spectrometer (Tokyo, Japan). All ^{1}H-NMR spectra were recorded in DMSO-d_6 solutions using tetramethylsilane as the internal standard. Dynamic light scattering (DLS) measurements were carried out using a DLS-8000 instrument (Otsuka Electrinics, Tokyo, Japan). An Ar ion laser (λ_0 = 488 nm) was used as the incident beam. The sample was prepared by direct mixing of pDNA solution and the polymer in Tris-HCl buffer (pH 7.4). The DNA concentration of the mixture was then adjusted to 23 μg cm^{-3}.

Cell Culture and Transfection

COS-1 cells (ca. 3 x 10^4 cells per well) were seeded prior to treatment in 24-well plates and grown for 24 h in DMEM (Gibco, Invitrogen Corp., Carlsbad, CA) containing 10% fetal calf serum (Hyclone Laboratories Inc., Logan, UT), penicillin (200 units/ml, ICN Biomedicals Inc., Aurora, OH), and streptomycin (200 mg/ml, ICN) in an atmosphere of 5% CO_2 at 37 °C. Transfections were performed with 0.5 μg of plasmid DNA (pGL3-control) in 24-multi well dishes in 0.2 ml of OPTI-MEM I (Gibco). After 3 h of incubation, the cells were washed once with PBS, and cultured in 1 ml of DMEM containing 10% fetal calf serum for an additional 48 h. The medium was removed and the cells were washed twice with PBS. The cells were lysed with 0.2 ml of cell lysis buffer (Promega, Madison, WI) and mixed by vortexing. The lysate was centrifuged at 15,000 rpm for 1 min at 4 °C and 5 μl of the supernatant was analyzed for luciferase activity using a Luminous CT-9000D (Dia-Iatron, Tokyo, Japan) luminometer. The relative light unit/s (RLU) were converted into the amount of luciferase (pg) using a luciferase standard curve, which was obtained by diluting recombinant luciferase (Promega) in lysis buffer. The protein concentrations of cells lysates were measured by Bio-Rad protein assay (BIO-RAD, Hercules, CA) using bovine serum albumin as a standard. The expressed luciferase represented the amount (mole quantity), which is standardized for total protein content of cell lysate. The data are presented as means±S.D. (n=5).

Cytotoxicity

Cytotoxicity was assessed by cell viability assay using WST-8 method (Dojindo, Kumamoto, Japan). COS-1 cells were seeded 24 h prior to treatment in 96-well plates at 5,000 cells per well. Cells were treated with the same conditions used for luciferase assays, with a volume of 6.2 μl of the transfection mixture including 0.124 μg of pDNA added to

each well. Cells were treated with the appropriate conditions for 3 h, washed once with PBS, and cultures in 50 μl of DMEM (Gibco) containing 10% fetal calf serum for an additional 24 h. Each well was added with 10 μl of WST-8 reagent (5 mmol/l). After 2 h of incubation at 37 °C, absorbance at 450 nm was read in a BIO-RAD microplate reader (Model 680). The data are presented as means±S.D. (n=5).

RESULTS AND DISCUSSION

Preparation of Cationic Star Polymers

Four kinds of cationic polymers, consisting of one linear polymer and three star polymers precisely controlled the degree of branching to 3, 4, and 6, were molecularly designed (Fig. 1). The polymers were synthesized by the iniferter living radical polymerization using respective initiators, multi-dithiocarbamate-derivatized benzenes, which were prepared corresponding to the degree of branching. As the monomer, a cationic vinyl monomer with tertiary amino residues, 3-(*N,N*-dimethylamino)propyl acrylamide was used. Since polymerization could proceed only during irradiation, the chain length of the polymers could be easily controlled by the irradiation condition and the composition of the solution. One linear and three kinds of star polymers with a molecular weight of about 18,000 with low polydispersity of about 1.5, irrespective of the degree of branching, were obtained. Therefore, the chain length in the polymers was set to about 6,000 with a degree of branching of 3, about 4,500 with a degree of branching of 4, and about 3,000 with a degree of branching of 6.

Polyplex Formation

When aqueous solutions of all obtained branched cationic polymers with same molecular weight were mixed with a Tris-HCl buffered saline of pDNA, marked high scattering intensity in quasi-elastic (dynamic) light scattering (DLS) measurements was immediately observed regardless of the degree of branching, indicating polyplexes formation from all cationic polymers. It was considered that the polyplexes formed by electrostatic interactions are same as other cationic polymeric vectors. The particle sizes of the polyplexes were measured using DLS. The DLS measurements showed that the cumulant diameter of the polyplexes was about 250 nm at a charge ratio less than 2/1 (vector/pDNA) and decreased to about 150 nm at a charge ratio more than 2.5/1(vector/pDNA). However, the particle

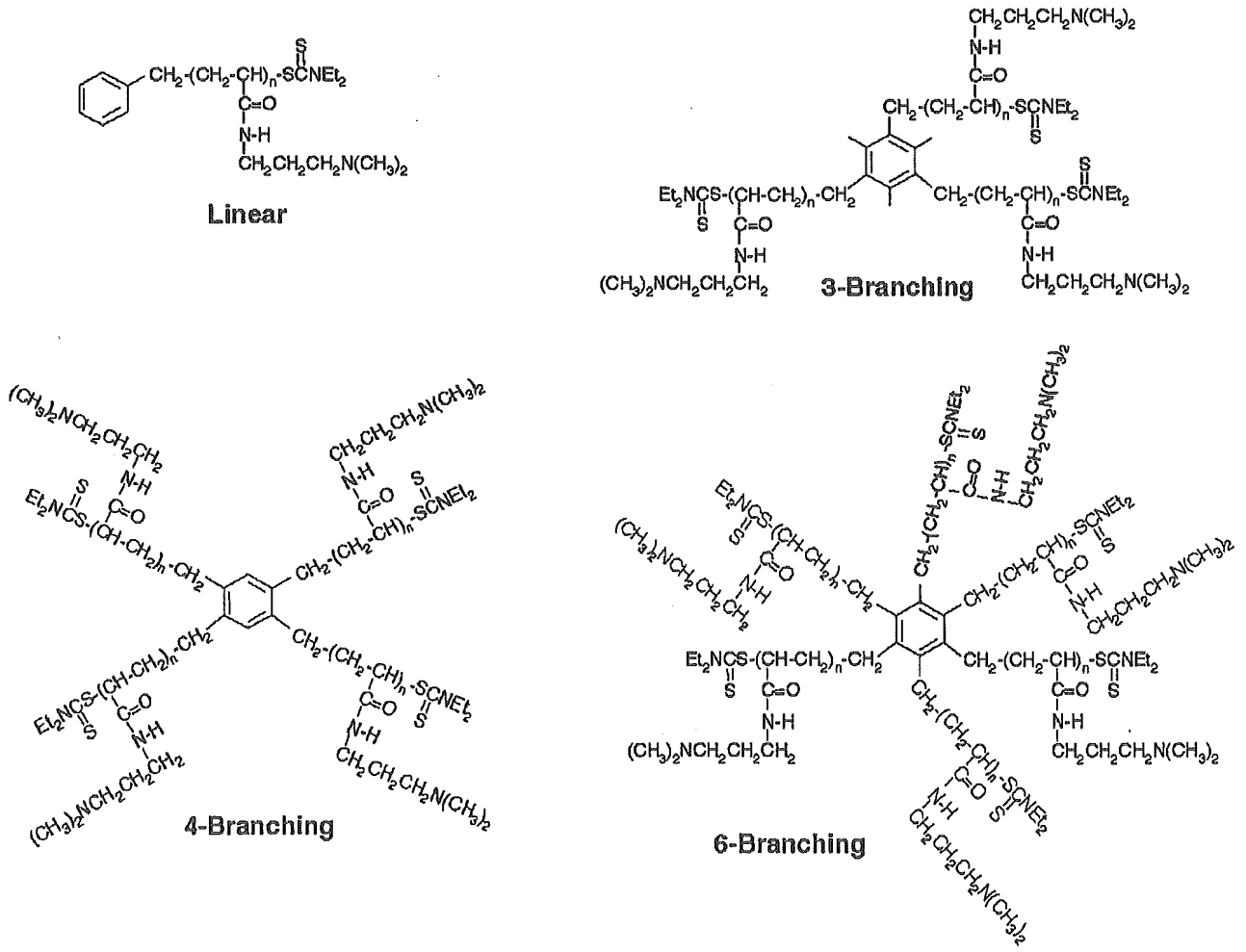

Fig. (1). Structural formulas of the star polymers, which were synthesized by iniferter-induced photo living radical polymerization of 3-(*N,N*-dimethylamino)propyl acrylamide from the respective multi-iniferters, *N,N*-diethyldithiocarbamate-derivatized benzenes.

sizes of the polyplexes were not significantly affected by the branching. In addition, ζ-potentials of pDNA polyplexes with the cationic polymers were measured to examine their electric property. The ζ-potential of the pDNA polyplexes was about +10 mV at a charge ratio more than 1/1(vector/pDNA). The difference in ζ-potential value between the polymers was little in each branching. Therefore, it can be said that there is little difference in physiochemical properties of the polyplexes produced from cationic polymers with different branching.

Cytotoxicity

Cytotoxicity of the pDNA polyplexes with the 6-branching polymer to COS-1 cells was studied by the cell survival rate using the WST-8 method. As shown in (Fig. 2) the cytotoxicity of the polyplexes was negligible up to a charge ratio of 5/1 (vector/pDNA). At charge ratios more than 5/1, the cytotoxicity was gradually reduced, and it was about 60% at a charge ratio of 20/1 (vector/pDNA).

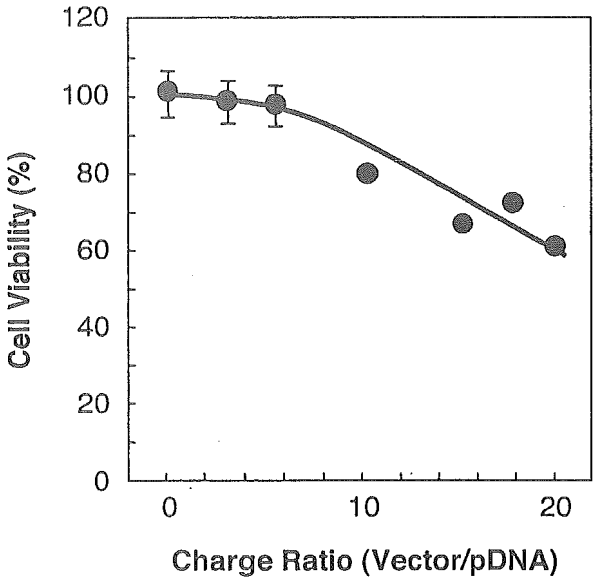

Fig. (2). Cytotoxicity of the polyplexes obtained immediately after mixing of DNA (pGL3-control) and 6-branching star polymer under the changing of a charge ratio (vector/pDNA), which was determined by cell viability assay of COS-1 cells using a WST-8 method. The data are presented as means±S.D. (n=5).

Gene Expression and Cell Viability

Gene transfer activity of the cationic polymers with same molecular weight of about 18,000 was examined and compared with that of ExGen 500 [35,36], which was one of major commercially available typical cationic polymeric vectors as a positive control. Figure 3 shows gene transfer activity of the cationic polymers at the charge ratio of 5/1 (vector/pDNA) in COS-1 cells. When pDNA alone was transfected, little luciferase activity was observed (data not shown). On the other hand, the luciferase was produced in all pDNA polyplexes. The enhancement of gene transfer activity in the use of the polyplexes may be due to acceleration of cellular uptake of pDNA polyplexes by

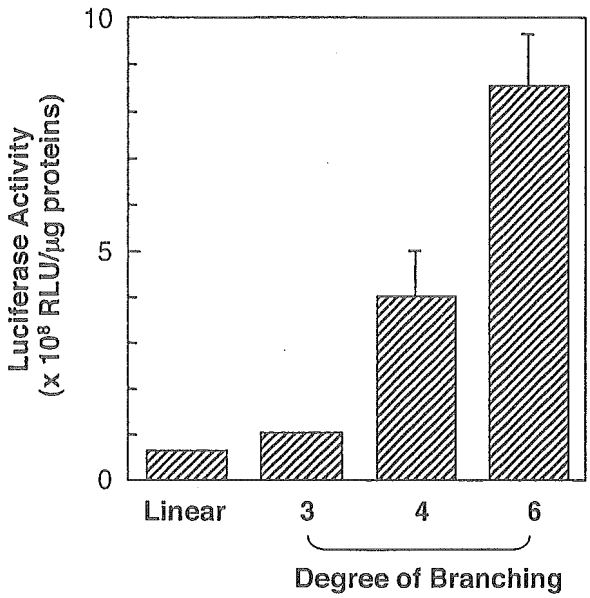

Fig. (3). Effect of branching of the star polymers on the level of luciferase gene transfer activity in COS-1 cells. COS-1 cells were treated with the polyplexes prepared by mixing of the star polymers and DNA (pGL3-control) under a charge ratio of 5/1 (vector/pDNA) 12 h after those preparation. The expression level was increased with increases in the degree of branching. The data are presented as means±S.D. (n=5).

endocytosis and endosomal release of the polyplexes by the proton sponge effect [37,38] in endosomes, similar to the other cationic polymers. The gene transfer activity of the pDNA polyplexes with the non-branched, linear cationic polymer was lowest, which was comparable with that of ExGen 500. However, the activity was increased by stage, corresponding to the degree of branching. The relative transfer activity to the linear polymer was about 2, 5 and 10 times in 3-, 4- and 6-branched polymers, respectively. As an increase in the degree of branching the transfer activity was almost exponentially increased. It can be said that the highly branched polymer called star vectors is useful for a gene delivery vector.

Cationic polymer-mediated transfection should overcome three major barriers for transfection, which includes binding of pDNA polyplexes to cell surface, endosormal release, and entry of pDNA into the nucleus. These barriers are strongly depended on the physicochemical properties of polyplexes such as net charge and particle size. Therefore, such properties markedly determine transfection efficiency. However, in the present study, transfection efficiency was strongly affected with the branching degree regardless of almost same physcochemical properties in pDNA polyplexes formed from the all branched polymers. The branching degree-dependent transfer activity changing may be estimated below. As an increase in the degree of branching the density of cationic charges in the branched polymers is increased. Higher charge density may affect the formation of higher compaction of pDNA polyplexes. The condensed pDNA polyplexes thus obtained may be stable in endosomes and also in aqueous media, which may prevent degradation

and aggregation of the polyplexes, respectively. Therefore, higher branching resulted in higher gene transfer activity.

The other star polymers as a gene delivery vector are easily designed by iniferter-based photo-living-radical polymerization. The composition of polymer chains can be determined by the kind of monomers, and the molecular weight by the irradiation time. Therefore, in addition to allowing design of the basic skeletal structure, the composition and length of polymer chains can be optimized as schematically shown in (Fig. 4). Changing the kind of monomers can control the composition of the polymer chains continuously or stepwise. To further increase the degree of branching, we will design the core molecules from benzene ring to naphthalene ring or combinations of benzene rings as multi-iniferters. Furthermore, formation of hyper branching structure by diverging of branching chains will be possible [34]. In the near future, the correlation between the three-dimensional structure in a star vector and the efficiency of gene expression will be clarified in detail.

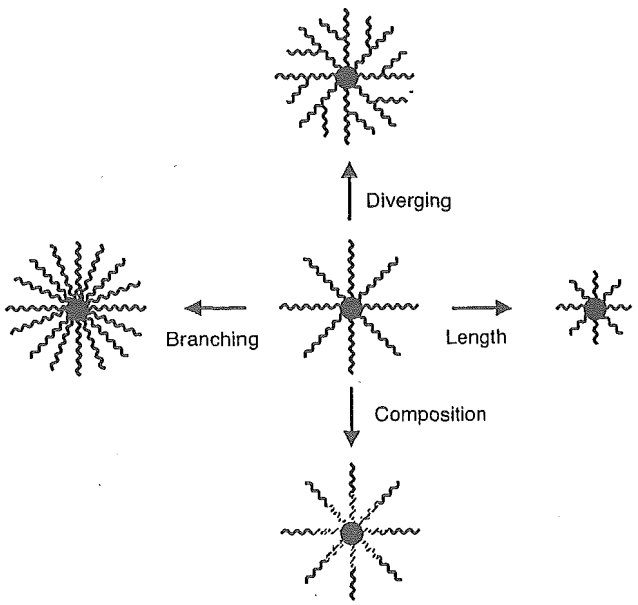

Fig. (4). Possibility in molecular design of various star polymers having different branching, diverging, chain length, or composition, which are based on iniferter-induced living radical polymerization.

ACKNOWLEDGEMENTS

This study was supported by "Research Grants for Advanced Medical Technology", "Human Genome, Tissue Engineering and Food Biotechnology", and "Aging and Health" from the Ministry of Health, Labor and Welfare of Japan, and by Grant-in-Aid for Scientific Research (B1-16390423) from the Ministry of Education, Science, Sports and Culture of Japan.

REFERENCES

[1] Felgner, P.; Barenholz, Y.; Behr, J.P.; Cheng, S.H.; Cullis, P.; Huang, L.; Jessee, F.J.; Seymour, L.; Szoka, F.; Thierry, A.R.; Wagner, E.; Wu, G. *Hum. Gene Ther.*, 1997, *8*(5), 511-2.

[2] Niidome, T.; Huang, L. *Gene. Ther.*, 2002, *9*(24), 1647-52.

[3] Thomas, M.; Klibanov, A.M. *Appl. Microbiol. Biotechnol.*, 2003, *62*(1), 27-34.

[4] Gebhart, C.L.; Kabanov, A.K. *J. Control Release*, 2001, *73*(2-3), 401-16.

[5] Nishikawa, M.; Huang, L. *Hum. Gene Ther.*, 2001, *12*(8), 861-70.

[6] Kichise, T.; Taguchi, S.; Doi, Y. *Appl. Environ. Microbiol.*, 2002, *68*(5), 2411-9.

[7] Zanta, M.A.; Boussif, O.; Adib, A.; Behr, J.P. *Bioconjug. Chem.*, 1997, *8*(6), 839-944.

[8] Diebold, S.S.; Kursa, M.; Wagner, E.; Cotton, M.; Zenke, M. *J. Biol. Chem.*, 1999, *274*(27), 19087-94.

[9] Kircheis, R.; Kichler, A.; Wallner, G.; Kursa, M.; Ogris, M.; Felzmann, T.; Buchberger, M.; Wagner, E. *Gene Ther.*, 1997, *4*(5), 409-18.

[10] Wojda, U.; Miller, J.L. *J. Pharm. Sci.*, 2000, *89*(5), 674-81.

[11] Li, S.; Tan, Y.; Viroonchatapan, E.; Pitt, B.R.; Huang, L. *Am. J. Physiol.*, 2000, *278*(3), L504-11.

[12] Kurisawa, M.; Yokoyama, M.; Okano, T. *J. Control. Release*, 2000, *69*(1), 127-37.

[13] Nagasaki, T.; Taniguchi, A.; Tamagaki, S. *Bioconjug. Chem.*, 2003, *14*(3), 513-6.

[14] Nakayama, Y.; Umeda, M.; Uchida, K. unpublished data.

[15] Hui, S.W.; Stoicheva, N.; Zhao, Y.L. *Biophys. J.*, 1996, *71*(2), 1123-30.

[16] Kuo, J.H.; Jan, M.S.; Sung, K.C. *Int. J. Pharm.*, 2003, *257*(1-2), 75-84.

[17] Petersen, H.; Kunath, K.; Martin, A.L.; Stolnik, S.; Roberts, C.J.; Davies, M.C.; Kissel. T. *Biomacromolecules*, 2002, *3*(5), 926-36.

[18] Zelikin, A.N.; Putnam, D.; Shastri, P.; Langer. R.; Izumrudov, V.A. *Bioconjug. Chem.*, 2002, *13*(3), *548-53.*

[19] Kunath, K.; von Harpe, A.; Fischer, D.; Petersen, H.; Bickel, U.; Voigt, K.; Kissel, T. *J. Control. Release.*, 2003, *89*(1), 113-25.

[20] Godbey, W.T.; Wu, K.K.; Mikos, A.G. *J. Biomed. Mater. Res.*; 1999, *45*(3), 268-75.

[21] Fischer, D.; Bieber, T.; Li, Y.; Elsasser, H.P.; Kissel, T. *Pharm. Res.*, 1999, *16*(8), 1273-79.

[22] Wightman, L.; Kircheis, R.; Rossler, V.; Carotta, S.; Ruzicka, R.; Kursa, M.; Wagner, E. *J. Gene Med.*, 2001, *3*(4), 362-72.

[23] Van de Wetering, P., Moret, E.E.; Schuurmans-Nieuwenbroek, N.M.E.; van Streenbergen, M.J.; Hennik, W.E. *Bioconjug. Chem.* 1999, *10*(4), 589-97.

[24] Tang, M.X.; Szoka, F.C. *Gene Ther.*, 1997, *4*(8), 823-32.

[25] Otsu, T.; Yoshida, M, *Makromol. Chem. Rapid Commun.*, 1982, *3*, 127-32.

[26] Otsu, T.; Yoshida, M.; Tazaki, T. *Makromol. Chem., Rapid Commun.*, 1982, *3*, 133-40.

[27] Otsu, T.; Matsunaga, T.; Doi, T.; Matsumoto, A.; *Eur. Polym. J.*, 1995, *31*, 67-78.

[28] Otsu, T.; Matsumoto, *Advances in Polymer Science*, 1998, *136*, 75-137.

[29] Matyjaszewski, K. Ed. *Controlled radical polymerization.* ACS Symposium Series 685 American Chemical Society: Washington, DC, 1998.

[30] Sawamoto, M.; Kamigaito, M. In *Polymer Synthesis; Materials Science and Technology Series*; VCH-Wiley: Weinheim, 1998; Chapter 1.

[31] Nakayama, Y.; Matsuda, T. *Macromolecules*, 1996, *29*(27), 8622-30.

[32] Nakayama, Y.; Matsuda, T. *Langmuir*, 1999, *15*(17), 5560-66.

[33] Higashi, J.; Nakayama, Y.; Marchant, R.E.; Matsuda, T. *Langmuir*, 1999, *15*(6), 2080-8.

[34] Nakayama, Y.; Sudo, M.; Uchida, K.; Matsuda, T. *Langmuir*, 2002, *18*(7), 2601-6.

[35] Ferrari, S.; Moro, E.; Pettenazzo, A.; Behr, J.P.; Zacchello, F.; Scarpa, M. *Gene Ther.*, 1997, *4*(10), 1100-6.

[36] Coll, J.L.; Chollet, P.; Brambilla, E.; Desplangues, D.; Behr, J.P.; Favrot, M. *Hum. Gene Ther.*, 1999, *10*(10), 1659-66.

[37] Boussif, O.; Zanta, M.A.; Behr, J.P. *Gene Ther.*, 1996, *3*(12), 1074-80.

[38] Sonawane, N.D.; Szoka, F.C. Jr.; Verkman, A.S. *J. Biol. Chem.*, 2003, *278*(45), 44826-31.

Received: July 01, 2004 Accepted: August 03, 2004

Photo-Control of the Polyplexes Formation between DNA and Photo-Cation Generatable Water-Soluble Polymers

Mariko Umeda[1,2], Mariko Harada-Shiba[3], Kingo Uchida[2] and Yasuhide Nakayama[1,*]

[1]*Department of Bioengineering, Advanced Medical Engineering Center, National Cardiovascular Center Research Institute, Osaka, Japan,* [2]*Department of Materials Chemistry, Faculty of Science and Technology, Ryukoku University, Shiga, Japan,* [3]*Department of Bioscience, National Cardiovascular Center Research Institute, Osaka, Japan*

Abstract: Photo-cation generatable water-soluble polymers (Mw: approximately 1 x 10^5) were prepared by radical co-polymerization of *N,N*-dimethylacrylamide and vinyl monomer of triphenylmethane leucohydroxide (malachite green), which generate a cation upon ultraviolet light (UV) irradiation at wavelengths of between 290 and 410 nm. The malachite green contents of the copolymers were 3.6 (0.4 mol %), 7.9 (0.7 mol %), and 15.0 (2.7 mol %) per molecule. When an aqueous solution of the photo-cationized copolymers generated by UV irradiation was mixed with a Tris-HCl buffer (pH 7.4) of DNA (pGL3-control plasmid), dynamic light scattering (DLS) measurements showed the formation of polyplexes between the cationic copolymers and anionic DNA by non-specific electrostatic interaction, which was visualized with a confocal laser scanning microscopy (CLMS). Their mean cumulant diameter was about 150 nm with low polydispersity irrespective of the malachite green content in the copolymers. In the copolymer with the lowest malachite green content, almost all of the amount of the polyplexes was maintained by repeated UV irradiation, but the amount gradually decreased in the dark at 37 °C due to dissociation of the polyplexes, synchronized with the neutralization of the cation form of malachite green. The photo-cation generatable copolymers designed here can undergo photo-induced formation of the polyplexes with DNA and thermal polyplex dissociation, which may be used as a model for a novel photo-induced gene delivery system into cells.

Keywords: Photo-induced polyplex formation, Photo-control, Photo-cation generatable polymer, Malachite green, Polyplex dissociation.

1. INTRODUCTION

Viral vectors with high gene transfection efficiency both *in vitro* and *in vivo*, such as adenovirus and retrovirus, have been widely used for gene therapy [1-8] since its first use for the treatment of adenosine deaminase (ADA) deficiency in 1990 [8]. However, since a fatal accident with an adenovirus vector in the USA in 1999, high safety standards have been required in the use of such vectors. Therefore, in recent years the development of non-viral vectors, which can be expected to have high biological safety, has been further accelerated. One major approach in the development of non-viral vectors is based on synthetic cationic polymers [9-20], including poly(ethylene imine) [13,14], poly-L-lysine [15,16], poly (amidoamine) dendrimer [17,18], and poly[(2-dimethyl-amino)ethyl methacrylate] [19,20], which can spontaneously form 'polyplexes' as a result of electrostatic interactions between the positively charged groups of the cationic polymers and the negatively charged phosphate groups of DNA. The cationic polymer-induced gene delivery systems have several advantages in addition to 1) high biological safety, and these are: 2) low costs, 3) ease of preparation and manipulation, and 4) no limitation of the size of transduced genes. However, the primary obstacle toward implementing a clinically available gene therapy using cationic polymers as vectors remains their extremely low efficiency in gene transfection *in vivo* compared with virus vectors.

It is strongly indicated that polyplexes are usually taken up by cells in endosormal compartments *via* endocytosis induced by non-specific electrostatic interactions between positively charged groups on the polyplex surface and negatively charged residues on the cell surface. When the polyplexes are released from the highly acidic endosormal compartment, and if the polyplexes can be easily dissociated, DNA released from the polyplexes will be more efficiently taken in by nuclei, resulting in higher transcription and gene expression. Therefore, the promotion of gene transfection may be improved by increasing: 1) the introduction of polyplexes into cells, 2) release of DNA from introduced polyplexes into the cytoplasm, and 3) delivery of DNA to nuclei. To enhance the introduction of polyplexes into cells, many research groups have attempted the introduction of targeting ligands such as galactose, mannose, transferrin, or antibodies into cationic polymers [19,21-25]. Such biochemical approaches have provided high gene expression. On the other hand, even using existing vectors, the promotion of gene transfection has been obtained by physical stimulation of transfection using electroporation, gene gun, ultrasound and hydrodynamic pressure [9,26,27]. These physicochemical approaches are very simple, and can be widely used.

Recently, a new gene delivery system, which can control the release of DNA, has been developed by the molecular design of polymeric vectors. For example, Yokoyama *et al.*

*Address correspondence to this author at the Department of Bioengineering, Advanced Medical Engineering Center, National Cardiovascular Center Research Institute, 5-7-1 Fujishiro-dai, Suita, Osaka 565-8565, Japan; Tel: +81-6-6833-5012; Fax: +81-6-6872-8090; E-mail: nakayama@ri.ncvc.go.jp

1567-2018/05 $50.00+.00

constructed a temperature-controlled gene expression system, in which a thermosensitive random copolymer, based on cationized poly(*N*-isopropylacrylamide) (PNIPAM), was synthesized as a thermoreactive vector [28]. Increased cellular uptake of the polyplexes, consisting of the cationized PNIPAM and DNA, at 37 °C and its disintegration by the reduction of temperature to 20 °C were demonstrated. A photo-controlled gene transfection system was proposed by Nagasaki *et al.* [29]. A photoreactive vector was designed, consisting of cationic lipids with an o-nitrobenzyl moiety as a photocleavable spacer. The DNA complex that had been taken up by the lipids was disintegrated by UV irradiation. In both systems external physical stimulation with temperature or light could promote enhancement of gene expression.

Malachite green is a well-known photochromic molecule that reversibly dissociates into ion pairs under ultraviolet light (UV) irradiation, producing intensely deep-green-colored triphenylmethyl cations and counter hydroxide ions within a few minutes (Fig. 2) [30,31]. The generated cations are stable under acidic condition. In our previous study, we synthesized water-soluble polyacrylamide-based copolymers with malachite green side chains, which could be immediately taken up into cells by non-specific electrostatic interactions due to conversion from the nonionic copolymers to polycations by UV irradiation [32]. The photo-generated cations slowly reverted to the original leucohydroxide species on cessation of the UV irradiation even under physiological temperature within approximately 1 h as shown in Fig. 2.

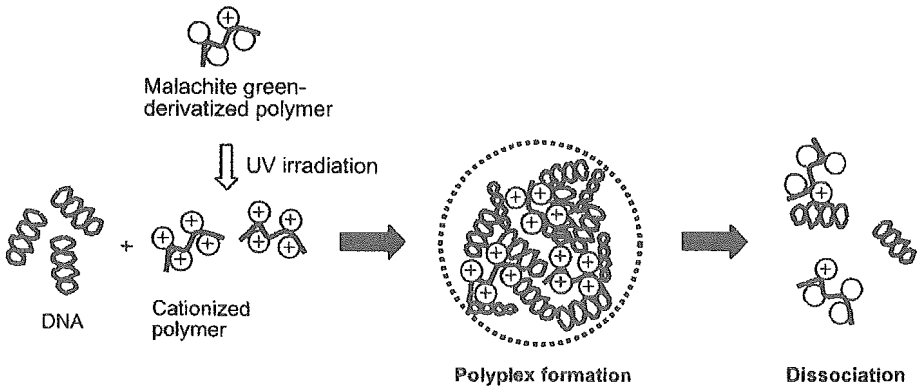

Fig. (1). Schematic illustration of the principle of photo-induced polyplex formation and its dissociation, both of which were based on the specific photochemical/thermal reactivity of the malachite green-derivatized water-soluble polymer.

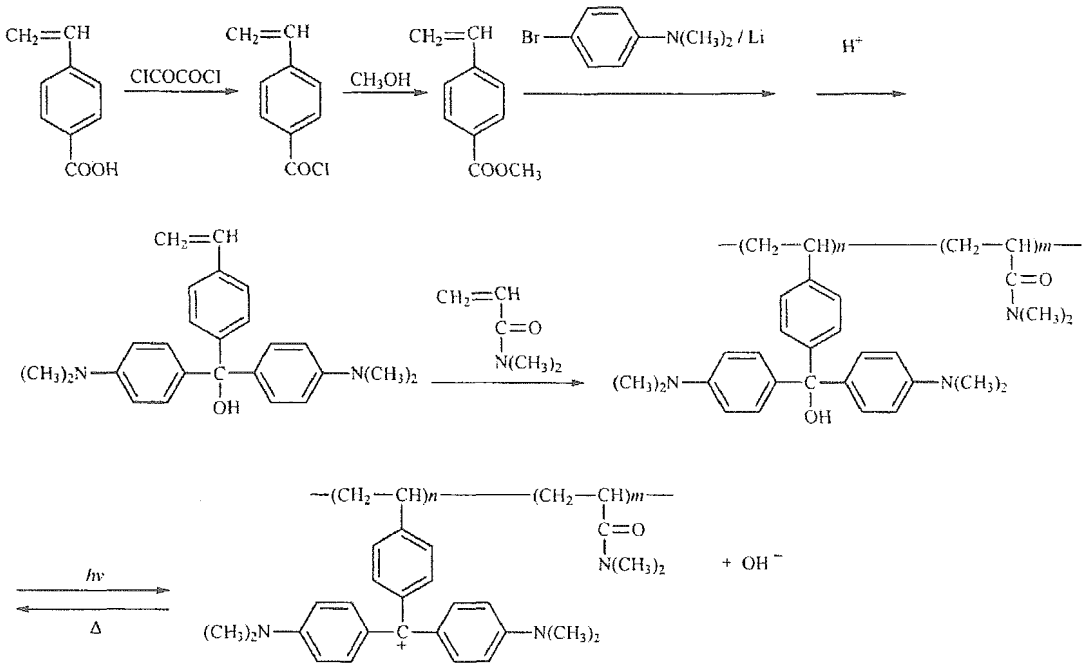

Fig. (2). Reaction scheme of the preparation of photo-cation generatable water-soluble copolymer, which is a radical copolymer of diphenyl(4-vinylphenyl)methane leucohydroxide and *N,N*-dimethylacrylamide. Chemical reaction in photoinduced dissociation of triphenylmethane leucohydroxide (malachite green) derivatized in the copolymer to triphenylmethyl cation and counter hydroxide ion and thermal recombination between them.

Therefore, if using the malachite green-derivatized polymers as a vector, it is expected that upon UV irradiation polyplexes can be formed from the photo-generated cationic polymers and DNA, and these can be dissociated by the time-dependent decrease in cation concentration in the dark (Fig. 1). In this study, water-soluble poly(*N,N*-dimethylacrylamide)-based copolymers with malachite green groups as side chains were synthesized (Fig. 2). Their photo-induced polyplex formation with DNA and thermal dissociation reactions were evaluated by measuring the light scattering intensity using a dynamic light scattering (DLS) measurement apparatus. The possibility of using the malachite green-derivatized polymers for a vector material in a novel photo-induced gene delivery system is discussed.

2. MATERIALS AND METHODS

2.1. Materials

4-Vinylbenzoic acid and 4-bromo-*N,N*-dimethylaniline were purchased from Tokyo Kasei Kogyo Co., Ltd. (Tokyo, Japan). Oxalyl chloride, *N,N*-dimethylacrylamide, 2,2'-azobis(isobutyronitrile) (AIBN), and *n*-butyl lithium hexane solution were purchased from Wako Pure Chemical Industries, Ltd. (Osaka, Japan). All other regents and solvents were obtained commercially and were purified by distillation.

2.2. Synthesis of Diphenyl(4-Vinylphenyl)methane Leucohydroxide [33]

Oxalyl chloride (21.4 g, 170 mmol) was added to 4-vinylbenzoic acid (5 g, 34 mmol) at less than 0 °C and stirred at room temperature for 8 h. After the oxalyl chloride was evaporated off under vacuum, dry methanol (50 mL) was added to the residue. Solvent evaporation from the reaction mixture afforded methyl 4-vinylbenzoate: 5.1 g (93%); ^{1}H NMR ($CDCl_3$): δ 7.99 (d, *J*=8.1 Hz, 2H, m-H of PhC=C), 7.46 (d, *J*=8.7 Hz, 2H, o-H of PhC=C), 6.75 (q, *J*=10.8 Hz, 1H, PhCH=C), 5.86 (d, *J*=17.4 Hz, 1H, cis-H of PhCH=CH_2), 5.38 (d, *J*=10.2 Hz, trans-H of PhCH=CH_2), 3.91 (s, 3H, $COOCH_3$).

4-Bromo-*N,N*-dimethylaniline (12.3 g, 61.7 mmol) was dissolved in anhydrous tetrahydrofuran (THF) (100 cm^3) and the solution was kept at –78 °C in a liquid nitrogen bath under an argon atmosphere. A hexane solution of butyllithium (BuLi) (48 mL, 77 mmol) was injected gradually into the THF solution with stirring. To the mixture was added dropwise a THF (70 cm^3) solution of methyl 4-vinylbenzoate (5 g, 30.8 mmol). The reaction mixture was allowed to warm slowly to room temperature and then stirred for an additional hour. After the reaction, the THF was evaporated off under vacuum and water (150 cm^3) was added to the residue. The aqueous phase was then neutralized by the addition of 0.1 mol dm^{-3} hydrochloric acid. Extraction with dichloromethane, followed by vacuum evaporation of the solvent, afforded a dark-green oily product of diphenyl(4-vinylphenyl)methane leucohydroxide **1**. Recrystallization of the crude product from methanol yielded a pale-green solid of **1** (42%). ^{1}H NMR (DMSO-d_6): δ 7.34 (d, *J*=9.0 Hz, 2H, *m*-H of PhC=C), 7.28 (d, *J*=9.0 Hz, 2H, *o*-H of PhC=C), 7.12 (d, 4H, *J*=9.0 Hz *o*-H of NPh), 6.74 (dd, *J*=10.8, 18.0 Hz, 1H, PhC*H*=C), 6.65 (d, *J*=8.1 Hz, 4H, *m*-H of NPh), 5.72 (d, *J*=16.2 Hz, 1H, *cis*-H of PhCH=CH_2), 5.21 (d, *J*=10.8 Hz, 1H, *trans*-H of PhCH=CH_2), 2.94 (s, 12H, -NCH_3).

2.3. Synthesis of Photo-cation Generatable Water-soluble Polymer [32]

The photo-cation generatable water-soluble polymers were prepared by radical copolymerization of diphenyl(4-vinylphenyl)methane leucohydroxide with *N,N*-dimethylacrylamide in benzene at 60 °C for 24 h, in a glass tube sealed after several freeze-pump-thaw cycles under vacuum. The total monomer concentration was set at 0.7 mol dm^{-3} (feed of diphenyl(4-vinylphenyl)methane leucohydroxide was changed from 0.1 to 0.5 mol % in the text), and α,α'-azobis(isobutyronitrile) (AIBN) was used as the initiator (0.5 mol % relative to the total monomer). The polymer, precipitated by addition of a large amount of ether, was separated from the solution by filtration. Reprecipitation was carried out sufficiently from the methanol solution to ether three times to exclude non-reacted monomer and initiator completely. The last precipitate was dried under a vacuum and stored in a dark desiccator. The molecular weight was determined by gel permeation chromatograph (GPC) analysis. The triphenylmethane leucohydroxide group contents were 3.6 (0.4 mol %), 7.9 (0.7 mol %), and 15.0 (2.7 mol %) per molecule, which was determined from the absorption spectrum using the absorption coefficient of malachite green carbinol base, which had a maximum absorption at a wavelength of 620 nm in an aqueous solution (ε = 6.7 x 10^4 $dm^3mol^{-1}cm^{-1}$). Polymerization yield was adjusted less than about 20 % to obtain copolymers with homogeneous composition. ^{1}H NMR ($CDCl_3$): δ 7.2-7.4 (Ph-C), 6.9-7.15 (*o*-H of NPh), 6.45-6.70 (*m*-H of NPh), 2.7-2.9 (PhNCH_3, CONCH_3), 1.1-1.6 (-CH_2-).

2.4. General Methods

Irradiation was carried out using a mercury-xenon arc lamp (L2859-01; Hamamatsu Photonics Inc., Shizuoka, Japan). The illumination wavelength ($290 < \lambda < 410$ nm) was selected with the aid of cutoff filters (UV-D33S, Toshiba, Tokyo, Japan). The light intensity, measured with a photometer (UVR-1, TOPCON, Tokyo, Japan), was fixed at 1.0 mW/cm^2. The absorption spectra were measured using a UV/visible light (VIS) spectrophotometer (UV-1700, Shimadzu, Kyoto, Japan). GPC analysis was carried out on a RI-8012 (TSK_{gel} α-3000 and α-5000, Toso, Tokyo, Japan) after calibration with standard poly(ethylene glycol) samples. The eluent was *N,N*-dimethylformamide. ^{1}H-NMR spectra were obtained on a Varian Gemini-300 (300 MHz) spectrometer (Tokyo, Japan). ^{1}H-NMR spectra were recorded in deuterated chloroform ($CDCl_3$) or dimethyl sulfoxide (DMSO-d_6) solutions using tetramethylsilane (TMS) as the internal standard. Dynamic light scattering (DLS) measurements were carried out using a DLS-8000 instrument (Otsuka Electrinics, Tokyo, Japan). An argon (Ar) ion laser (λ_0 = 488 nm) was used as the incident beam. The sample was prepared by direct mixing of the DNA solution and polymer in Tris-HCl buffer (pH 7.4). The DNA concentration of the mixture was then adjusted to 23 μg cm^{-3}. The fluorescence image of the polyplexes was obtained using a confocal laser scanning microscope (CLSM, 543 nm, Radiance2100, Bio-Rad Lab., Hercules, CA).

Table 1. Preparation of Photo-Cation Generatable Water-Soluble Copolymers and their Composition

Feed of MG[a] monomer (mol %)	Yield (%)	MG[a] content (mol %)	Mn^b ($x10^4$)	polydispersity	number of MG[a] / molecule
0.1	22	0.4	9.1	2.6	3.6
0.2	20	0.7	11.4	2.1	7.9
0.5	17	2.7	5.9	2.3	15.0

Polymerization conditions: initiator, AIBN; [monomer]/[initiator] = 200; Solvent; benzene; [monomer] = 0.7 mol/l; temp., 60°C; Polym. Time, 17 h. [a] MG means malachite green. [b] Number-average molecular mass determined by gel-permeation chromatography (PEO standard). [c] Determined by absorption spectra at 620 nm.

3. RESULTS

3.1. Preparation and Physical Properties of Photo-cation Generatable Water-soluble Polymers

Photo-cation generatable water-soluble polymers were prepared by free radical copolymerization of *N,N*-dimethylacrylamide with the photo-dissociable monomer, diphenyl(4-vinylphenyl)methane leucohydroxide according to the previously reported method [32] (Fig. 2). The content of the photodissociable group, triphenylmethane leucohydroxide, in the copolymers was determined by absorption spectroscopy using the absorption coefficient at an absorption maximum (620 nm) of a malachite green carbinol base. Table 1 summarizes the preparation conditions and compositions of the copolymers. ^{1}H NMR spectra indicated that by repetition of sufficient reprecipitation no non-reactive monomer and initiator was detected completely in the all polymers obtained. Polymer yield was adjusted under about 20 % to obtain homogeneous copolymers with narrow distribution of copolymerization ratio. The malachite green contents in the copolymers of molecular weight about 0.6-1x10^5, were 3.6 (copolymerization ratio; 0.4 mol %), 7.9 (0.7 mol %) and 15.0 (2.7 mol %) units per molecule.

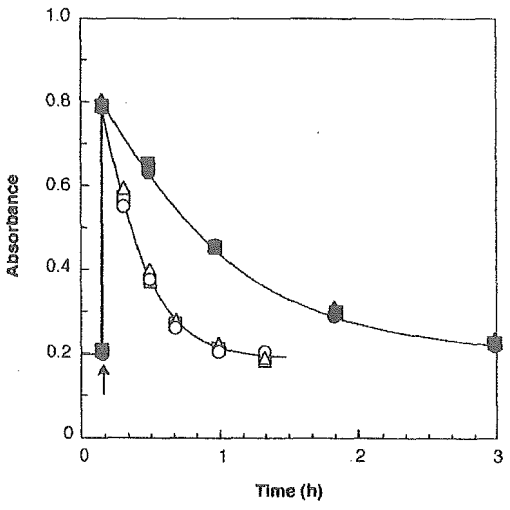

Fig. (3). Absorbance changes at 620 nm in aqueous solutions of photo-cation generatable water-soluble copolymers (malachite green content per molecule, 3.6: ○; 7.9: △; 15.0: □), and the polyplexes from the photo-cation generatable water-soluble copolymer (malachite green content, 3.6: ●; 7.9: ▲; 15.0: ■) and DNA (pGL3-control plasmid, 0.5 μg). Arrow indicates the time of UV irradiation for 2 min.

Aqueous solutions of the three copolymers at pH 7.4 and 37 °C were light green before UV irradiation. Upon UV irradiation at a wavelength of between 290 and 410 nm, the aqueous solutions spontaneously turned to deep green with an increase in absorption at 620 nm (Fig. 3) and exhibited a considerably elevated pH to about 8.5. These were attributed to the generation of a triphenylmethyl cation according to Fig. 2. Within 1 min of UV irradiation almost all malachite green groups were converted to the cationic form. On cessation of the UV irradiation the absorption at 620 nm reverted to the initial level (one quarter of the maximum level) within about 1 h regardless of the malachite green contents in the copolymers, indicating that three quarters of all cationic forms slowly reverted to the original leucohydroxide, nonionic form. Therefore, one quarter of the malachite green groups were present as cations at equilibrium state at pH 7.4 and 37 °C.

3.2. Polyplex Formation and Degradation

When DNA was added to Tris-HCl buffered solution of the cationic copolymers produced from the malachite green-derivatized copolymers by UV irradiation, a marked high scattering intensity in DLS measurements was immediately observed regardless of the malachite green contents of the copolymers (Table 2). In contrast, low scattering intensities were detected in saline solutions of DNA or the copolymers with or without UV irradiation, or even after mixing of DNA with the copolymers without UV irradiation (Table 2). For all copolymers, the scattering intensity was highest at C/A ratios between 0.5 and 1. An example in the use of the copolymer, with a malachite green content of 15.0, is shown in Fig. 4. The larger number and size of the particles caused a larger scattering intensity. Therefore, it can be said that the photo-cation-generated copolymers produced polyplexes upon mixing with DNA at the appropriate mixing ratio. The cumulant analysis of the DLS measurements showed that the diameter of the polyplexes produced at C/A ratios ranging from 0.25 to 5 was about 150 nm with low polydispersity (about 0.4) (Fig. 4). In addition, the polyplexes formation was visualized by fluorescent microscopic image because the malachite green is a fluorescent dye, where almost all polyplexes observed by exposure to light of wavelength 543 nm were in spherical shape (Fig. 5).

Upon incubation at 37 °C of the polyplex solutions, prepared from the copolymer with the lowest malachite green-content, the scattering intensities gradually decreased up to 3

Table 2. Scattering Intensity of Tris-HCl Buffered (pH 7.4) DNA and/or Malachite Green-Derivatized Copolymer (Malachite Green Content; 15.0) with or without UV Irradiation

Run	Solution condition			Scattering intensity
	DNA[a]	copolymer[a]	*hν*[a]	
1	-	-	-	49.1 ± 21.8
2	O	-	-	158.2 ± 27.3
3	-	O	-	169.1 ± 12.4
4	-	O	O	174.5 ± 38.2
5	O	O	-	916.3 ± 299.9
6	O	O	O	2345.2 ± 97.3

[a]Key: o, presence; -, absence.

h (Fig. 6), which was well synchronized with the change in absorbance of the malachite green groups (Fig. 3). After 3 h of incubation the scattering intensity had declined to one half that obtained immediately after mixing of the photo-cationized copolymer and DNA. In addition, in this time the cumulant diameter of the polyplexes decreased from approximately 150 to 100 nm. However, little change in the scattering intensity and the cumulant diameter were observed in the high malachite green content (7.9 and 15.0) copolymers (Fig. 6) despite a decrease in the amount of cations in the copolymer (Fig. 3). These results indicated that the polyplexes were formed immediately upon mixing of the photo-cationized copolymers and DNA for all the copolymers studied, and gradually dissociated only in the lowest malachite green-content copolymer to release of DNA without any damages, which was confirmed by the observation of the shift of DNA electrophoretic migration in agarose gel (data not shown).

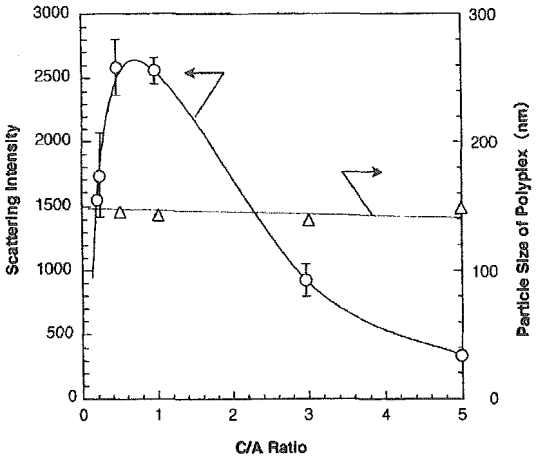

Fig. (4). Scattering intensity (O) and cumulant diameter (Δ) of an aqueous solution of the polyplexes prepared by mixing of photo-cation generatable water-soluble copolymer (malachite green content per molecule, 15.0) and DNA (pGL3-control plasmid, 0.5 μg) in different ratios.

When 1-min UV irradiation of the polyplex solutions was repeated every 10 min the absorbance at 620 nm was maintained to some extent for the lowest malachite green content copolymer for up to 2 h (Fig. 7), indicating that almost all cationized malachite green groups existed without conversion

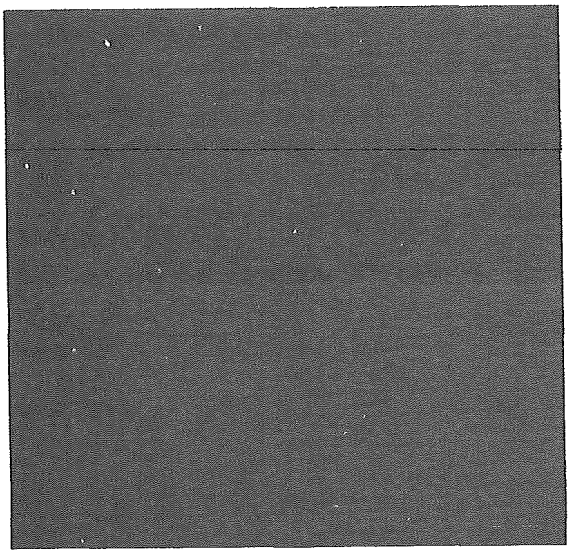

Fig. (5). Fluorescence microscopic image of the polyplexes from the photo-cation generatable water-soluble copolymer (malachite green content per molecule, 15.0) and DNA at C/A ratio of 1. Bar=10 μm.

to the nonionic form due to the action of the intermittent UV irradiation. Simultaneously, under the same UV irradiation conditions, the scattering intensity derived from the polyplexes was also maintained at the initial value to some extent (Fig. 6), indicating the dissociation of the polyplexes was prevented under UV irradiation. However, upon cessation of UV irradiation the scattering intensities started to spontaneously decrease, due to disappearance of the cations (Fig. 6). Therefore, it can be said that the formation and dissociation of the polyplexes were photochemically controlled.

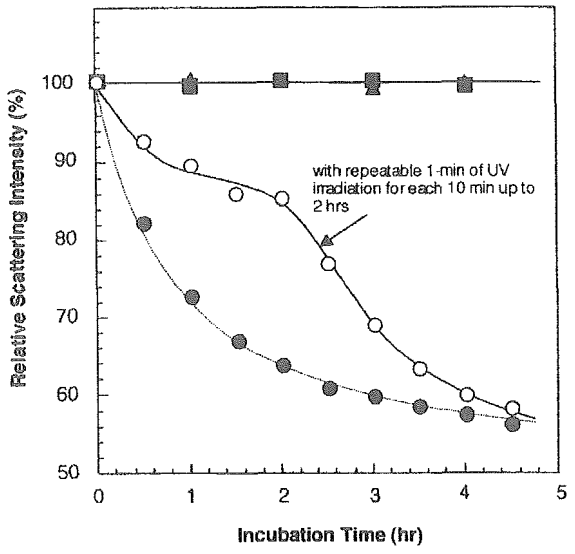

Fig. (6). Changes in scattering intensity of an aqueous solution of the polyplexes prepared by mixing photo-cation generatable water-soluble copolymer (malachite green content per molecule, 3.6: ○ and ●; 7.9: ▲; 15.0: ■) with 2-min of UV-irradiation, and DNA (0.5 μg) at C/A ratio of 1. (○): 1-min of UV irradiation was performed repeatedly every 10 min up to 2h.

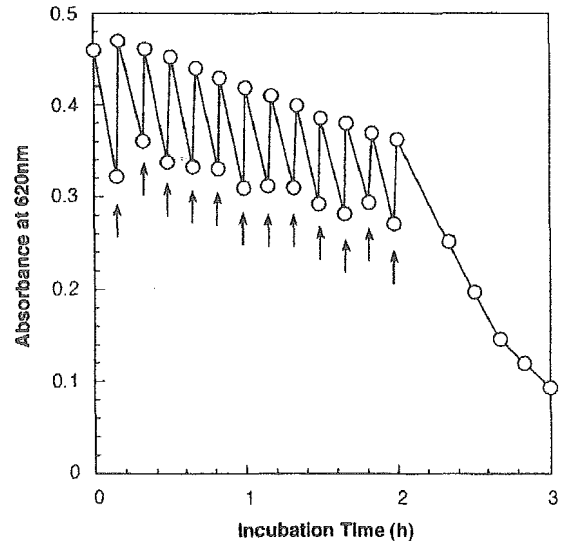

Fig. (7). Change in absorbance at 620 nm of an aqueous solution of the polyplexes prepared by mixing of photo-cation generated water-soluble copolymer (malachite green content; 3.6) and DNA at C/A ratio of 1. Arrows indicate the time of 1-min UV irradiation.

4. DISCUSSION

In this study, as a model compound as a vector for a proposed new gene delivery system a photoreactive water-soluble polymer derivatized with a photochromic compound, malachite green was molecularly designed [30,31]. Since malachite green can reversibly generate a cation as shown in (Fig. 2), the malachite green-derivatized water-soluble polymers developed here can be reversibly converted from a nonionic to cationic form by UV irradiation. Therefore, the following three functions will be expected when using the polymers as a vector. Namely, cationization upon UV irradiation induces 1) acceleration of the formation of polyplexes with DNA and their subsequent cellular uptake due to enhancement of electrostatic interactions. Since malachite green exists as a stable cation under highly acidic conditions, the polyplexes are stably maintained in endosomal compartments. Therefore, 2) DNA can be protected from enzymatic degradation and hydrolysis in the endosome. If the polyplexes are released into the pH-neutral cytoplasm, thermal deionization of cations will occur, which causes: 3) dissociation of the polyplexes, resulting in the release of DNA. The last function, 3), may provide the most effective enhancement of the gene delivery to nuclei in addition to the others 1) and 2), both of which are usually present in other cationic copolymers designed as vectors.

The malachite green-derivatized water-soluble polymers synthesized in this study were radical copolymers of malachite green-derivatized vinyl monomer and a water-soluble monomer, *N,N*-dimethylacrylamide. Poly(*N,N*-dimethylacrylamide), is a widely used medical material, for biocompatible surface coatings for medical devices [34,35] and for the modification of drugs [36]. Malachite green has been studied as a functional material in drug delivery systems [32]. In addition, an affinity chromatography of DNA was developed by using A.T-base-pair-specific affinity of the chloride derivative of malachite green [37]. There have been few reports showing toxicity in these materials. In our previous study, there was little significant difference between the control and endothelial cells (ECs) after treatment with the copolymers synthesized here, regardless of the presence of UV irradiation in the exclusion test of trypan blue [32]. In addition, the long-range viability and integrity of the ECs were not altered from the control upon incubation with the copolymers at the concentration less than 1 mg/mL, which is about 10 times larger than that used in standard *in vitro* transfection experiments [32]. On the other hand, about 70 % of cell viability was reported in Exgen500, which is polyethylenimine, one of the commercially avairable cationic polymer vectors. Therefore, it can be said that the copolymers were biocompatible with little cytotoxicity. The copolymers will be excluded from the cells without any cellular damages because they can not degraded by hydrolysis *et al.*

In our previous study, cationized malachite green-derivatized water-soluble copolymers generated by UV irradiation were taken up in cells by electrostatic interactions, whereas the non-ionic form of the copolymers before irradiation displayed no detectable interaction with cell membranes [32]. The strength of interaction was increased by the amount of malachite green residues introduced into the copolymers and the irradiation time, i.e., the amount of generated cations. To obtain high interaction strength with cells, copolymers with many malachite green residues are required. However, to maintain the water-solubility of copolymers, the content of malachite green residues must be less than several mol % due to their hydrophobicity.

In this study, 3 kinds of photoreactive copolymers with 3.6 (content of malachite green residues; 0.4 mol %), 7.9 (0.7 mol %), and 15 (2.7 mol %) of malachite green groups per molecule were prepared. In all copolymers, upon mixing with DNA aqueous solutions and after irradiation there was a marked increase in scattering intensity (Table 2), indicating the generation of polyplexes by non-specific electrostatic interaction. The formation of the polyplexes was also confirmed by observation of CLSM. The diameter of the obtained polyplexes was approximately 150 nm, irrespective of the malachite green content (Fig. 4). The amount of malachite green cations in the polyplexes returned to the initial level, i.e., the level prior to irradiation, (about 25% of the entire malachite green groups) in about 3 h (Fig. 3). Since the amount of cations in an aqueous solution of the copolymers alone returned to the initial level in about 1 h (Fig. 3), binding of malachite green cations with hydroxyl anions may have been inhibited in the polyplexes. The scattering intensity of the polyplex solution prepared from the lowest malachite green content copolymer 3 h after irradiation was reduced to approximately 50% that immediately after irradiation (Fig. 6), indicating dissociation of the polyplexes. If the dissociation of the polyplexes occurs in the cytoplasm, gene delivery to nuclei will be enhanced.

Only the lowest malachite green content copolymer polyplexes were dissociated (Fig. 6). About 4 cations remained in the highest malachite green content copolymer approximately 3 h after irradiation and were sufficient to form polyplexes. Deionization of malachite green cations was prevented to some extent by repeated irradiation at intervals (Fig. 7). Therefore, maintaining the amount of cations through continuous irradiation could control the condition of the complex. These results suggested that generation and dissociation of the complex could be controlled by irradiation. However, amount of cations was gradually decreased even intermittent irradiation, which may be due to decreasing of malachite green molecules by photochemical side reaction, resulted in prevention of maintenance of stable polyplexes.

In the copolymer with 3.6 malachite green residues per molecule, in principle, less than 1 cation exists in a molecule in the dark. Therefore, it is expected that the copolymer cannot bind to more than 1 DNA molecule, indicating that no polyplex can be generated. However, complete dissociation of the polyplexes could not be achieved even in the use of the copolymer. This may be due to the relatively high polydispersity of the copolymer. To completely dissociate the polyplexes in neutral solution, it is necessary to design a new malachite green-derivatized polymer, in which the number of malachite green units is strictly controlled to 2-4 per molecule, or a functional molecule that is completely deionized in neutral solution. With regard to the former material, we have been investigating synthesis by controlled polymerization methods, such as living radical polymerization. With regard to the latter, since malachite green is converted into cations by dissociation of hydroxyl anions, it tends to be in the leuco form at equilibrium under alkaline conditions because of suppression of dissociation (Fig. 2). Therefore, even in the polyplex with the highest malachite green content, the scattering intensity was reduced to about 25% at pH 9 24 h after irradiation, and to about 10% at pH 10 within about 1 h after irradiation, whereas little change in the scattering intensity was observed at pH 6 (Fig. 8). At pH 10, the change in scattering intensity was well correlated with that in absorbance (Fig. 8). In other words, complete deionization of malachite green led to almost complete dissociation of the complex. The other approach to complete dissociation of the polyplexes is the synthesis of leuconitrile derivates of malachite green as model compounds, which could exist in a complete non-ionic form before irradiation, and would not be affected by the pH of the solution.

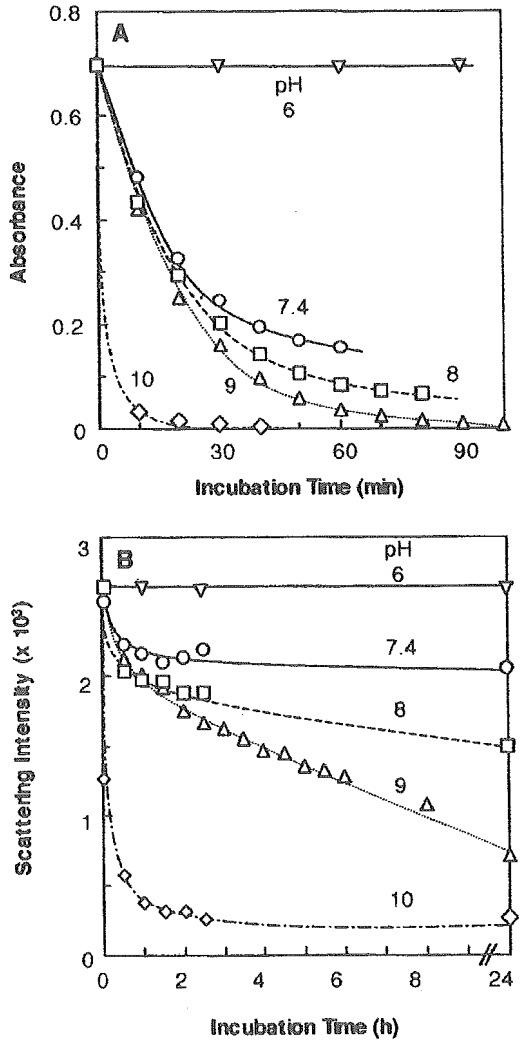

Fig. (8). Changes in absorbance (A) and scattering intensity (B) of an aqueous solution of the polyplexes of photo-cation generatable water-soluble copolymer (malachite green content per molecule, 15.0) and DNA at C/A ratio of 1 at different pHs.

This study indicated that generation and dissociation of polyplexes of water-soluble polymer and DNA was controlled to some extent using the specific photo/thermoreactivity of malachite green (Fig. 1). It can be said that a new model for gene delivery system into cells has been demonstrated. For the next stage of this study, we are planning to

examine *in vitro* transfection efficiency. It is highly expected that only by mixing with the malachite green-derivatized copolymers after irradiation DNA will deliver effectively to inside of cells by endocytosis. The degree of delivery will be controlled easily by irradiation time and malachite green content. In addition, thermal dissociation ability of the photogenerated polyplexes after escaping from endosomes will promote DNA delivery to nuclei, which will cause the enhancement of transfection efficiency. Such study will be reported in the near future.

ACKNOWLEDGEMENTS

The authors would like to thank Ms. Keiko Jinno for her expert technical assistance in this study. This work was supported by "Research Grants for Advanced Medical Technology", "Human Genome, Tissue Engineering and Food Biotechnology", and "Aging and Health" from the Ministry of Health, Labur and Welfare of Japan, and by Grant-in-Aid for Scientific Research (B1-16390423) from the Ministry of Education, Science, Sports and Culture of Japan.

REFERENCES

[1] Somia, N.; Verma, I.M. *Nat. Rev. Genet.*, **2000**, *1*, 91-99.
[2] Anderson, W.F. *Nature*, **1998**, *392*, 25-30.
[3] St George, J.A. *Gene Ther.*, **2003**, *10*, 1135-1141.
[4] Miyake, S.; Makimura, M.; Kanegae, Y.; Harada, S.; Sato, Y.; Takamori, K.; Tokuda, C.; Saito, I. *Proc. Natl. Acad. Sci. USA*, **1996**, *93*, 12320-1324.
[5] Wang, Q.; Finer, M.H. *Nat. Med.*, **1996**, *6*, 714-716.
[6] Kotin, R.M. *Hum. Gene Ther.*, **1994**, *5*, 793-801.
[7] Finer, M.H.; Dull, T.J.; Qin, L.; Farson, D.; Roberts, M.R. *Blood*, **1994**, *83*, 43-50.
[8] *Hum. Gene Ther.*, **1990**, *1*, 327-362.
[9] Niidome, T.; Huang, L. *Gene Ther.*, **2002**, *9*, 1647-1652.
[10] Thomas, M.; Klibanov, A.M. *Appl. Microbiol. Biotechnol.*, **2003**, *62*, 27-34.
[11] Gebhart, C.L.; Kabanov, A.K. *J. Control. Release*, **2001**, *73*, 401-416.
[12] Nishikawa, M.; Huanl, L. *Hum. Gene Ther.*, **2001**, *12*, 861-870.
[13] Oh, Y.K.; Suh, D.; Kim, J.M.; Choi, H.G.; Shin, L.; Ko, J.J. *Gene Ther.*, **2002**, *9*, 1627-1632.
[14] Boussif, F.; Lezoualc'h, M.A.; Zanta, M.D.; Mergny, D.; Scherman, B.; Demeneix, J.P.; Behr, C. *Proc. Natl. Acad. Sci. USA*, **1995**, *92*, 7297-7301.
[15] Itaka, K.; Yamauchi, K.; Harada, A.; Nakamura, K.; Kawaguchi, H.; Kataoka, K. *Biomaterials*, **2003**, *24*, 4495-4506.
[16] Jeon, E.; Kim, H.D.; Kim, J.S. *J. Biomed. Mater. Res.*, **2003**, *66A*, 854-859.
[17] Kihara, F.; Arima, H.; Tsutsumi, T.; Hirayama, F.; Uekama, K. *Bioconjug. Chem.*, **2003**, *14*, 342-350.
[18] Arima, H.; Kihara, F.; Hirayama, F.; Uekama, K. *Bioconjug. Chem.*, **2001**, *12*, 476-484.
[19] Lim, D.W.; Yeom, Y.I.; Park, T.G. *Bioconjug. Chem.*, **2000**, *11*, 688-695.
[20] Cherng, J.Y.; van de Wetering, P.; Talsma, H.; Crommelin, D.J.; Hennink, W.E. *Pharm. Res.*, **1996**, *13*, 1038-1042.
[21] Zanta, M.A.; Boussif, O.; Abdennaji, A.; Behr, J.P. *Bioconjugate. Chem.*, **1997**, *8*, 839-944.
[22] Diedold, S.S.; Kursa, M.; Wagner, E.; Cotton, M.; Zenke, M. *J. Biol. Chem.*, **1999**, *274*, 19087-19094.
[23] Kircheis, R.; Kichler, A.; Wallner, G.; Kursa, M.; Ogris, M.; Felzmann, T.; Buchberger, M.; Wagner, E. *Gene Ther.*, **1997**, *4*, 409-418.
[24] Wojda, U.; Miller, J.L. *J. Pharm. Sci.*, **2000**, *89*, 674-681.
[25] Li, S.; Tan, Y.; Viroonchatapan, E.; Pitt, B.R.; Huang, L. *Am. J. Physiol.* **2000**, *278*, L504-L511.
[26] Hui, S.W.; Stoicheva, N.; Zhao, Y.L. *Biophys. J.*, **1996**, *71*, 1123-1130.
[27] Kuo, J.H.; Jan, M.S.; Sung, K.C. *Int. J. Pharm.*, **2003**, *257*, 75-84.
[28] Kurisawa, M.; Yokoyama, M.; Okano, T. *J. Control. Release*, **2000**, *69*, 127-137.
[29] Nagasaki, T.; Taniguchi, A.; Tamagaki, S. *Bioconjugate. Chem.*, **2003**, *14*, 513-516.
[30] Bertelson, R.C. in Brown, G.H. (ed.), *Photochromism. Techniques of Chemistry*, Vol. III, Wiley-Interscience, New York, **1971**, pp. 294.
[31] Irie, M.; Kungwatchakun, D. *Macromolecules*, **1986**, *19*, 2476.
[32] Nakayama, Y.; Matsuda, T. *J Control Release*, **2003**, *89*, 213-224.
[33] Kimura, K.; Yokota, G.; Yokoyama, M.; Uda, R.M. *Macromolecules*, **2001**, *34*, 2262-2268.
[34] Nakayama, Y.; Takatsuka, M.; Matsuda, T. *Langmuir*, **1999**, *15*, 1667-1672.
[35] Matsuda, T.; Nagase, J.; Ghoda, A.; Hirano, Y.; Kidoaki, S.; Nakayama, Y. *Biomaterials*, **2003**, *24*, 4517-4527.
[36] Masuda, T.; Nakayama, Y. *J. Med. Chem.*, **2003**, *46*, 3497-3501.
[37] Bunemann, H.; Muller, W. *Nucleic. Acids. Res.*, **1978**, *5*, 1059-1074.
[38] Erbacher, P.; Bettinger, T.; Brion, E.; Coll, J.L.; Plank, C.; Behr, J.P.; Remy, J.S. *J. Drug Target.*, **2004**, *12*, 223-236.

Received: September 29, 2004 Accepted: December 22, 2004

ELSEVIER

Atherosclerosis xxx (2005) xxx–xxx

ATHEROSCLEROSIS

www.elsevier.com/locate/atherosclerosis

The effect of ezetimibe on serum lipids and lipoproteins in patients with homozygous familial hypercholesterolemia undergoing LDL-apheresis therapy

Akira Yamamoto [a,*], Mariko Harada-Shiba [a], Michinori Endo [b], Norio Kusakabe [c,1], Tsuneo Tanioka [c,2], Hiroshi Kato [d], Takashi Shoji [e,3]

[a] *National Cardiovascular Center Research Institute, Suita, Osaka, Japan*
[b] *Seisuikan Hospital, Susono, Shizuoka, Japan*
[c] *Shin-Osaka Iseikai Clinic, Osaka, Japan*
[d] *Nishi-Kobe Medical Center, Kobe, Japan*
[e] *Beppu National Hospital, Beppu, Japan*

Received 12 January 2005; received in revised form 21 June 2005; accepted 27 June 2005

Abstract

LDL-apheresis is now commonly used as the only practical treatment for homozygous familial hypercholestreolemia (homozygous FH). However, even when applying apheresis therapy, the use of a drug or drugs is recommended to suppress the rapid rebound of cholesterol, which usually takes place after each apheresis procedure, and keep the LDL-cholesterol level within or near the optimal range for as long as possible. In this study, the usefulness of ezetimibe, a novel cholesterol-lowering drug, in enhancing the efficacy of apheresis therapy was evaluated in six Japanese patients with homozygous FH undergoing LDL-apheresis in combination with atorvastatin or simvastatin. With the exception of one patient, significant decreases in LDL-cholesterol at 2 weeks after each apheresis procedure were obtained during the period from 4 to 12 weeks of treatment, with an average reduction rate of 9.0% and a range of 4.3–12.6%. This corresponds to a suppression of rebound by approximately 36 mg/dl, from 391 to 355 mg/dl on average, in LDL-cholesterol values. Although the effect is not very strong, ezetimibe nevertheless appears to be a useful drug in combination with statins for those with homozygous FH undergoing LDL-apheresis.

Keywords: LDL-apheresis; Homozygous familial hypercholesterolemia; Ezetimibe; Treatment of hyperlipidemia; Combination therapy of familial hypercholesterolemia

1. Introduction

Most cases of heterozygous familial hypercholesterolemia (heterozygous FH) can now be adequately treated with a combination drug therapy including hydroxymethylglutaryl coenzyme A (HMG-CoA) reductase inhibitors (statins) as the first choice drug [1]. In contrast, homozygous FH still remains an intractable disease due to its resistance to drug therapy [2], and LDL-apheresis is currently the only practical way of treating such patients [3–5]. However, as the severe rebound of cholesterol that occurs after each apheresis procedure diminishes the effect of this therapy [5], there is a need for suitable agents that can suppress such an acute rebound. Recently a novel cholesterol-lowering drug with a particular mechanism of blocking the cholesterol absorption at the brush border of the intestine has been developed [6,7]. Because the functional site of ezetimibe is different from LDL-receptors, it was expected that the drug would be effective in lowering cholesterol in homozygous FH. A

* Corresponding author. Present address: Health Care Facilities for the Aged, Minoh Life Plaza, 5-8-2 Kayano, Minoh, Osaka 562-0014, Japan. Tel.: +81 72 727 9530; fax: +81 72 727 3598.
E-mail address: ymmt-a@juno.dti.ne.jp (A. Yamamoto).
[1] Kusakabe Clinic, Ikeda, Osaka.
[2] Yukokai Hospital, Ibaragi, Osaka.
[3] Nakatsu City, Nakatsu, Oita.

0021-9150/$ – see front matter © 2005 Elsevier Ireland Ltd. All rights reserved.
doi:10.1016/j.atherosclerosis.2005.06.039

report from a clinical trial carried out in America, Europe and South Africa showed that the drug lowered LDL-cholesterol almost to the same extent as in patients with ordinary primary hypercholesterolemia; a 20.5% additional reduction in patients under treatment with atorvastatin or simvastatin at a dose of 80 mg/day with a consistent reduction in LDL-cholesterol being obtained regardless of LDL-apheresis [8]. However, the patients in the above trial were not stratified by LDL-apheresis. Furthermore, there is a wide rage of geneotype in FH. Previous studies have shown that there is a large variation in the efficacy of atorvastatin among patients with homozygous FH undergoing LDL-apheresis [9,10]. In this study, we therefore tried to see if ezetimibe would be useful in suppressing the rebound of cholesterol in patients with homozygous FH of the receptor-negative type under LDL-apheresis treatment combined with statin therapy.

2. Subjects and methods

2.1. Patients

Six homozygous FH patients undergoing LDL-apheresis treatment every 2 weeks were enrolled in the study (Table 1). All patients had receptor-negative phenotype almost completely lacking the LDL affinity binding to fibroblasts or mononuclear cells. Among the six patients, Cases 3–1 and 4–1 were sisters and Cases 2–1 and 2–2 were brother and sister. The original total cholesterol level at the first visit to hospitals or lipid clinics was 695 ± 115 mg/dl, and the average total cholesterol level before each apheresis procedure was 373 ± 59 mg/dl. Atorvastatin was used at a dose of 10–40 mg/day (10 mg dose in Case 2–1, 20 mg dose in Cases 3–1, 3–2 and 4–1, 40 mg dose in Case 2–2), while simvastatin was prescribed in Case 5–1 at a dose of 10 mg/day. Probucol was used in combination in 4 cases at a dose of 500 or 1000 mg/day (500 mg/day in Cases 3–2 and 5–1, 1000 mg/day in Cases 3–1 and 4–1). Ezetimibe was given at a dose of 10 mg/day after a meal once every day for 12 weeks.

2.2. LDL-apheresis

LDL-apheresis was carried out using the affinity chromatography technique with a dextran sulfate–cellulose column (Liposorber System MA-01; Kaneka Corporation; Osaka) (two patients) or the double membrane filtration technique (KM 8500 or 8800 equipped with EVAL-4A new type, Kuraray Co., Osaka, or Plasauto 1000 equipped with Plasmaflo, Asahi Medicals, Tokyo) (three patients) [11]. A consistent volume of blood plasma (3000–6000 ml depending on the individual patient) was treated at each procedure. Heparin was regularly used as an anticoagulant.

2.3. Therapy schedule

For the first 4 weeks of prechallenge observation, each patient remained on their conventional apheresis regimen including any drug(s) prescribed. They were asked to keep a regular life style during the course of prechallenge observa-

Table 1
Patient demographies

Patient no.	Sex, age	LDL receptor activity[a] (%)	TC[b] at first visit	Complications	Regular anti-lipidemic agents	Other cardiovascular drug(s)	LDL-C[c] at the start of the study period
2–1	F, 26	Negative (0)	806	IHD	Atorvastatin, 10 mg	–	423
2–2	M, 28	Negative (0)	822	Hypertension, IHD, aortic stenosis	Atorvastatin, 40 mg	Ca-channel blocker ARB β-blocker	421
3–1	F, 63	Negative (0)	748	Hypertension, stable angina, aortic steno-regurgitation, carotid artery stenosis, aortic aneurysm, cervical spondylosis	Atorvastatin, 20 mg, probucol, 1000 mg, eicosapentaemic acid (EPA), 1200 mg	Ca-channel blocker nitrate aspirin	418
3–2	F, 23	Negative (0)	672	–	Atorvastatin, 20 mg, probucol, 500 mg	–	282
4–1	F, 66	Negative (9)	661	Angina pectoris, cataract, carotid artery stenosis	Atorvastatin, 20 mg, probucol, 1000 mg, EPA, 1800 mg	Nicorandil β-blocker aspirin	325
5–1	M, 24	Negative (0)	700	Hypertension, stable angina, arteriosclerotic retinopathy, aortic steno-regurgitation	Simvastatin, 10 mg, probucol, 500 mg	Nitrate β-blocker aspirin	370

[a] Activity on lymphocytes: % of the average value of normal individuals.
[b] Total serum cholesterol (mg/dl).
[c] Low density lipoprotein cholesterol (mg/dl).

tion and the treatment (ezetimibe) period. After the prechallenge observation period, patients were given ezetimibe at a constant dose of 10 mg/day for 12 weeks. Compliance with drug administration was checked by the attending physician each time patients visited the clinic. This was almost 100%, except for one patient (Patient 5–1), who forgot to take the drug occasionally (5 days in total) during the period from the 7th to the 11th week. The compliance rate in this patient over the whole study period was 93.5%.

2.4. Lipoprotein and lipid analysis

Serum or plasma lipid values (total cholesterol:TC, HDL-cholesterol:HDL-C, triglycerides:TG and LDL-cholesterol:LDL-C) were measured at the Hachioji Laboratory of SRL Teijin Laboratories (Tokyo), where the measurement of the major lipid components was controlled indirectly by CDC through the Lipid Reference Laboratory, Osaka Medical Center for Health Science and Promotion [12]. TC and TG were measured enzymatically. HDL-cholesterol and LDL-cholesterol were measured by a newly developed homogeneous method applying an enzymatic–colorimetric assay in the presence of specific detergents, Cholestest HDL [13] and Cholestest LDL [14]. Apolipoproteins were measured turbidimetrically using corresponding antibodies [15].

Serum lipid levels were measured before the start and at the end of each apheresis procedure. Values obtained before each apheresis procedure (2 weeks after the previous treatment) were used to evaluate the effect of ezetimibe.

Defects in LDL-receptors in our patients were estimated by measuring the receptor activity on blood monocytes by flow-cytometric assay [16].

2.5. Monitoring adverse effects

Adverse events were monitored during the whole trial period. Clinical signs, symptoms and laboratory data (biochemical measurements of plasma components, hematology and urinalysis) were checked at least every 4 weeks.

2.6. Statistical analysis

The average, standard deviation and the confidence interval (CI) for the percent change (%) from before administration of ezetimibe to the measurement times at 2, 4, 6, 8, 10 and 12 weeks after initiation of the treatment period were calculated. Over-time changes in the measurements at the above time points were analyzed according to the mixed effect model of repeated measurements, where the effect measured by time was defined as fixed effect and the effect in individual subjects as variate effect. If the by-time effect was significant, comparison between before administration and the effect at subsequent time points was tested by the Dunnett's method.

3. Results

3.1. Validity of samples

In one of the patients (Patient 3–2), no data were judged as satisfying the validation criteria due to the irregularity of the apheresis procedure (intervals and treated blood volume) and also inconsistencies in dietary habits during the summer season. Accordingly, the data from this patient were excluded in the analysis of the efficacy, but were included in the analysis of adverse effects. Treatment conditions were also inconsistent in another patient (Patient 5–1) and only data at 6 weeks were judged to be valid. In Patient 3–1, data at 12 weeks were excluded due to the same reason.

3.2. Changes in serum lipid levels

Pretreatment levels of serum lipids and changes in TC, LDL–C, HDL–C and TG in five patients are summarized in Table 2.

LDL-C levels, the primary endpoint of this study, showed significant decreases in all of the five patients for whom efficacy data were available. They were analyzed by use of a mixed effect model of repeated measurements, and the point of measurement was found to have significant effect. Following this finding, the baseline measurement was compared with subsequent measurements by the Dunnett's method. Only one patient (Patient 3–1) showed a remarkable reduction in LDL-C at 2 weeks of the ezetimibe treatment, while in the other four patients, the reduction rates obtained at 2 weeks were remarkably smaller than the values obtained from the later weeks of the treatment; the difference was statistically significant by Dunnett's procedure. The average reduction rates in the period from 4 to 12 weeks of treatment in individual patients were 4.3–12.6% with an average of 9.0% for all patients (Table 3).

Table 2
Changes in LDL-cholesterol, total cholesterol, triglycerides and HDL-cholesterol following treatment with ezetimibe

	LDL-cholesterol	Total cholesterol	Triglycerides	HDL-cholesterol
Pretreatment level (mg/dl)	391.5 ± 43.4	474.5 ± 67.4	107.3 ± 52.8	30.7 ± 8.6
On completion of treatment (mg/dl)	354.6 ± 47.4	432.5 ± 79.2	113.6 ± 61.4	28.3 ± 7.5
Percent change (%)	−9.57	−9.07	18.78	−7.58
95% CI	−14.11 ~ −5.03	−17.43 ~ −0.72	−42.51 ~ 80.06	−18.98 ~ 3.82

Average ± standard deviation (five patients).

Table 3
Percent changes in LDL-cholesterol in individual patients during treatment with ezetimibe

Treatment period	Patient no.				
	2–1	2–2	3–1	4–1	5–1
2 weeks	7.48	−3.80	−15.62	−2.67	–
4 weeks	−5.51	−4.99	−9.88	−10.06	–
6 weeks	−3.15	−7.13	−8.21	−8.52	−10.0
8 weeks	−12.36	−9.74	−10.60	−14.68	–
10 weeks	−3.15	−1.43	−21.83	−10.37	–
12 weeks	2.76	−12.59		−11.29	–
Average during the period from 4 to 12 weeks	−4.28	−7.18	−12.63	−10.98	−10.0

The level of LDL-C in five patients before the start of the ezetimibe treatment was 391 ± 43 mg/dl on average, while the value at the end was 355 ± 48 mg/dl, the rate of change being −9.6% with a 95% confidence interval ranging between −14.1 and −5.03%. The rebound of LDL-C after an apheresis procedure (increase in LDL-C 2 weeks after completing an apheresis procedure) was calculated in three of the five patients and the values were −17, −29 and −57 mg/dl. One of our patients (Case 2–2) was administered atorvastatin 40 mg/day (maximum dose approved for Japanese). However, the effect of ezetimibe (7.2% reduction in LDL-cholesterol) was no more remarkable than the other patients who were given a smaller dose of atorvastatin or simvastatin).

TC values also showed significant decreases, with a pretreatment average value of 475 ± 68 mg/dl and an average value at the end of the treatment in individual patients of 433 ± 79 mg/dl (−9.1%). TG values did not show any remarkable changes. HDL-C showed a tendency to decrease, although the difference from the pretreatment level was not statistically significant; 7.6% reduction with a 95% confidence interval ranging between −19.0 and +3.8% (Table 2). The change in HDL-C showed the same pattern as LDL-C, with the reduction rate at 2 weeks being much less than that in later weeks and this difference was shown to be statistically significant by the Dunnett's procedure.

None of the other lipid parameters, VLDL-C, RLP-C, PL, FFA, apolipoproteins A-I, A-II, B, C-II, C-III, E and Lp(a), showed remarkable changes.

3.3. Adverse effects

Adverse effects occurring in more than one of the six patients following treatment with ezetimibe included nausea (three patients), and fatigability, cough and albuminuria (two patients). Adverse effects, whose relation to the drug could not be denied, were found in three patients; nausea 1, fatigability 2, cough 1, anorexia 1, increase in liver enzymes (AST and ALT) 1 and albuminuria 1. All the adverse effects were slight to mild. There were no remarkable changes in vital signs.

4. Discussion

Ezetimibe is a unique cholesterol-lowering drug, that exerts its function by inhibiting the absorption of cholesterol at the brush border of the intestine with Niemann-Pick C1 like 1 protein as a target of its action [17]. Clinical studies have shown that the drug is effective in reducing LDL-cholesterol by nearly 20% with monotherapy [6,7] and useful in achieving the goal of NCEP guidelines in combination with statins [18,19].

Homozygous FH is extremely resistant to drug therapy. According to Raal et al., atorvastatin or simvastatin at a large dose succeeded in reducing LDL-cholesterol from 15 mmol/l (about 600 mg/dl) to 10.9 mmol/l (about 440 mg/dl). However, increasing the dose above 80 mg/day did not result in any further reduction, which suggests a plateau effect in their patients [20]. Although the effect of ezetimibe in lowering LDL-cholesterol may be limited due to the induction of cholesterol synthesis in the liver [21] in a somewhat similar way to the effect of bile acid sequestering agents [22,23], it is worth testing its effect in homozygous FH as no antilipidemic drugs other than probucol [24] can exert their cholesterol-lowering effect in patients with homozygous FH. Atorvastatin has been shown to exert its effect at a relatively high dose and to be useful in assisting the efficacy of LDL-apheresis [9]. However, the effect is virtually limited to the receptor-defective type with a remnant LDL-receptor activity, and only a very small number of patients with the receptor-negative type do respond to treatment with atorvastatin due to the complete lack of LDL-receptor activity [10].

Our present study showed that ezetimibe suppressed the rebound of LDL-cholesterol after apheresis to some extent, with an average 9% reduction in LDL-cholesterol levels after 4 weeks. A report from clinical trials carried out in America, Europe and South Africa showed that ezetimibe lowered LDL-cholesterol almost to the same extent as in patients with ordinary primary hypercholesterolemia; a 20.5% additional reduction in patients under treatment with atorvastatin at a dose of 80 mg/day [8]. In our study, patients with homozygous FH of the receptor-negative type undergoing LDL-apheresis were registered. In the study in America, Europe and South Africa [8], a variety of mutations in LDL-receptors